

Title	Intraoperative dorsal language network mapping by using single-pulse electrical stimulation(Dissertation_全文)
Author(s)	Yamao, Yukihiro
Citation	Kyoto University (京都大学)
Issue Date	2014-03-24
URL	http://dx.doi.org/10.14989/doctor.k18180
Right	I am indebted to the journal “ Human Brain Mapping ” for publishing to the Kyoto University Research Information (“ KURENAI ”).Refer to the following URL for the abstract. http://onlinelibrary.wiley.com/doi/10.1002/hbm.22479/abstract
Type	Thesis or Dissertation
Textversion	ETD

Acknowledgement

I am indebted to the journal “Human Brain Mapping” for publishing to the Kyoto University Research Information (“KURENAI”).

Refer to the following URL for the abstract.

<http://onlinelibrary.wiley.com/doi/10.1002/hbm.22479/abstract>

Intraoperative dorsal language network mapping by using single-pulse electrical stimulation

Yukihiro Yamao¹, Riki Matsumoto², Takeharu Kunieda¹, Yoshiaki Arakawa¹, Katsuya

Kobayashi³, Kiyohide Usami³, Sumiya Shibata¹, Takayuki Kikuchi¹, Nobukatsu

Sawamoto³, Nobuhiro Mikuni⁴, Akio Ikeda², Hidenao Fukuyama⁵ and Susumu

Miyamoto¹

1 Department of Neurosurgery, Kyoto University Graduate School of Medicine

2 Department of Epilepsy, Movement Disorders and Physiology, Kyoto University

Graduate School of Medicine

3Department of Neurology, Kyoto University Graduate School of Medicine

4 Department of Neurosurgery, Sapporo Medical University School of Medicine

5 Human Brain Research Center, Kyoto University Graduate School of Medicine

Corresponding to: Riki Matsumoto & Takeharu Kunieda, Kyoto University Graduate

School of Medicine, Kyoto, Japan

54, Shogoin Kawahara-cho, Sakyo-ku, Kyoto, 606-8507, Japan

tel & fax: +81-75-751-3772 & +81-75-751-9416

e-mail: matsumot@kuhp.kyoto-u.ac.jp (RM), kuny@kuhp.kyoto-u.ac.jp (TK)

A short title: Intraoperative language network mapping

Keywords: awake craniotomy; cortico-cortical evoked potentials; subcortico-cortical evoked potentials; dorsal language network; arcuate fasciculus

Abbreviations: AF = arcuate fasciculus; AG = angular gyrus; AL = anterior perisylvian language area; CCEP = cortico-cortical evoked potential; DWI = diffusion weighted image; ECoG = electrocorticogram; ES = electrical stimulation; IFGop = pars opercularis of inferior frontal gyrus; IFGor = pars orbitalis of inferior frontal gyrus; IFGtr = pars triangularis of inferior frontal gyrus; ITG = inferior temporal gyrus; MEP = motor evoked potential; MFG = middle frontal gyrus; MTG = middle temporal gyrus; PL = posterior perisylvian language area; ROI = region of interest; SCEP = subcortico-cortical evoked potential; SMG = supramarginal gyrus; STG = superior temporal gyrus; WAB = Western Aphasia Battery

Abstract

The preservation of language function during brain surgery still poses a challenge. No intraoperative methods have been established to monitor the language network reliably.

We aimed to establish intraoperative language network monitoring by means of cortico-cortical evoked potentials (CCEPs). Subjects were six patients with tumors located close to the arcuate fasciculus (AF) in the language-dominant left hemisphere.

Under general anesthesia, the anterior perisylvian language area (AL) was first defined by the CCEP connectivity patterns between the ventrolateral frontal and temporoparietal area, and also by presurgical neuroimaging findings. We then monitored the integrity of the language network by stimulating AL and by recording CCEPs from the posterior perisylvian language area (PL) consecutively during both general anesthesia and awake condition. High-frequency electrical stimulation (ES) performed during awake craniotomy confirmed language function at AL in all six patients. Despite an amplitude decline ($\leq 32\%$) in two patients, CCEP monitoring successfully prevented persistent language impairment. After tumor removal, single-pulse ES was applied to the white matter tract beneath the floor of the removal cavity in five patients, in order to trace its

connections into the language cortices. In three patients in whom high-frequency ES of the white matter produced naming impairment, this “eloquent” subcortical site directly connected AL and PL, judging from the latencies and distributions of cortico- and subcortico-cortical evoked potentials. In conclusion, this study provided the direct evidence that AL, PL and AF constitute the dorsal language network. Intraoperative CCEP monitoring is clinically useful for evaluating the integrity of the language network.

Introduction

The preservation of brain functions during surgery still poses a challenge in patients with brain tumors at or close to the eloquent areas. Motor evoked potentials (MEPs) have become one of the gold standard measures for monitoring the motor function in tumor and epilepsy surgery, since MEPs can indicate the integrity of the whole motor network: the motor cortices and the output pathway, the pyramidal tract [Macdonald, 2006]. The online, sequential recording of MEPs is of great clinical significance, since it can be performed under general anesthesia in patients with tumors at or close to the motor cortex or the pyramidal tract. On the contrary, no intraoperative methods have been established to monitor language function under general anesthesia. Therefore, intraoperative monitoring during awake craniotomy is often required to evaluate language function when the tumor is located at or around the language cortex or its white matter pathways.

Electrical stimulation (ES) during awake craniotomy has been developed by introducing a biphasic current-constant pulse and optimizing the intraoperative tasks [Berger et al., 1989; Whitaker and Ojemann, 1977]. After propofol was introduced in

awake craniotomy in early 1990's, functional mapping with ES during awake craniotomy has become popular all over the world [July et al., 2009; Silbergeld et al., 1992]. High-frequency ES is commonly performed to identify the eloquent cortices such as the language area around tumors. In addition to the functional cortical mapping, the "eloquent" language fibers, namely the association fibers related to language function, have been extensively investigated with ES in pioneering work by Duffau [Duffau, 2008; Duffau et al., 2005]. However, these cortical- and subcortical ES methods could map only part of the language network, namely, the language cortex itself, or some (i.e., stimulus site) of the language fibers. As a result, even during awake craniotomy, no methods have yet been established to monitor the integrity of the language network during surgery, as opposed to MEPs for the motor network.

Recently, the development of diffusion tractography has enabled us to visualize the *in vivo* dissection of large white matter pathways in the living human brain. This noninvasive technique is widely applied for the preoperative evaluation of neurosurgery to trace major white matter pathways related to important brain functions, e.g., the pyramidal tract and the arcuate fasciculus (AF). It should be noted, however,

that these white matter pathways are solely determined by the calculated anisotropic diffusion of water molecules, and thus the technique itself does not probe their functional properties [Mori and van Zijl, 2002]. This limitation should be acknowledged, especially when the tracts representing the association fibers are traced into the cortices, since the terminations cannot be completely traced with this technique because of technical limitations such as the low signal-to-noise ratio at and around the cortices and fiber-crossings. Probabilistic diffusion tractography has been developed to overcome these limitations [Behrens et al., 2007], but it would be prudent to obtain complementary supporting evidence for clinical application to neurosurgery.

We have recently developed the *in vivo* electrical tract-tracing method using cortico-cortical evoked potentials (CCEPs) [Matsumoto et al., 2004]. In an extraoperative setting for presurgical evaluation of epilepsy surgery, single-pulse ES was applied directly to the cortex, and CCEPs were recorded from the remote cortex through cortico-cortical connections. In contrast to high-frequency (50 Hz) ES that aimed to define brain functions such as language, this invasive tract-tracing method with single-pulse ES provides us with a unique opportunity to track functional

connectivity among different cortices electrophysiologically. This method has successfully delineated the language, motor, and parietofrontal networks [Enatsu et al., 2013; Matsumoto et al., 2012; Matsumoto et al., 2007; Matsumoto et al., 2004]. CCEP studies are relatively easy to perform: for each averaged result from a given stimulus site, it takes only 1–2 min with little patient cooperation; the chance of provoking seizures is extremely low, and the reproducibility or reliability of the data is very high [Matsumoto et al., 2007]. Therefore, the CCEP technique could be applicable in an intraoperative setting to identify and monitor the functionally important networks at or in the vicinity of lesions such as tumors.

The objective of the present study was to apply this single-pulse ES technique and to establish it as a novel intraoperative method to monitor the language network. Similarly to the intraoperative MEP recording, we aimed to monitor the degree of integrity of the language network by stimulating Broca's area and by recording CCEPs from Wernicke's area sequentially during the resection of the tumor located around the AF. In addition, during awake craniotomy, we attempted to obtain data supporting that the connections we traced by CCEPs and diffusion tractography are indeed involved in

language function; 50 Hz ES was applied to the cortex and the white matter tracts to define their function, and 1 Hz ES was applied to the deeply seated tract in order to trace its cortical terminations at the language cortices by recording the cortical evoked responses [subcortico-cortical evoked potentials (SCEPs)].

Materials and Methods

Subjects

Subjects were six patients (mean age 33 years, ranging from 19 to 44; 2 males) with brain tumors located close to the perisylvian language areas in the language-dominant left hemisphere. Language dominance was defined by Wada test, which was performed using intra-carotid infusion of propofol [Takayama et al., 2004]. On neurological examination, four patients were unremarkable, one showed mild hemiparesis, and the other was found to have mild cognitive impairment and right upper quadrantanopsia. None of the patients showed any language impairment preoperatively, which was evaluated by the Japanese version of the Western Aphasia Battery (WAB) in five patients and formal neurological examination in one patient. Four patients had a history

of partial seizures. The pathology of the tumor was a dysembryoplastic neuroepithelial tumor in two patients and glioma in four (diffuse astrocytoma, anaplastic astrocytoma, oligodendroglioma, and WHO grade II-III astrocytoma; Table 1).

Language function was evaluated with the WAB before and after surgery.

Postoperative evaluation was performed within 6 weeks of surgery. For those who showed language impairment in the postoperative evaluation, a follow-up evaluation was performed 2 or 3 months after surgery.

Informed consent was obtained from all patients, and the present study was approved by the Kyoto University Graduate School and Faculty of Medicine, Ethics Committee (IRB C573).

In all patients, awake craniotomy was performed. A wide craniotomy exposing the distal end of the Sylvian fissure, the frontal operculum, and the posterior part of the superior and middle temporal gyri (STG and MTG) was performed under general anesthesia using propofol. After the patients awoke, ES was performed mainly under local anesthesia.

Experimental paradigm for language mapping and preservation

Since the clinical goal was to preserve language function during surgical procedures, we attempted to map the dorsal pathway of the language network [Hickok and Poeppel, 2004]. By using 50 Hz and single-pulse ES for functional cortical/subcortical mapping and electrical tract-tracing, respectively, we aimed to map and monitor the dorsal language pathway in individual patients in the following order:

- 1) Before surgery, we localized the language cortex and the underlying white matter pathway (AF) by using functional magnetic resonance imaging (fMRI) and probabilistic diffusion tractography.
- 2) Under general anesthesia, we applied single-pulse ES to cortical regions around the anterior perisylvian language area (AL) that was localized based on anatomic criteria or by using fMRI before surgery. Based on the CCEP distribution in the lateral temporoparietal area, i.e., the CCEP connectivity pattern between the AL and the posterior perisylvian language areas (PL), we determined the stimulus site (i.e., the putative AL) most appropriate for online CCEP monitoring. The integrity of the

dorsal language pathway was then evaluated by online sequential CCEP monitoring during surgical procedures.

- 3) After the patient woke up, language assessment with batteries and CCEP recording was sequentially performed during surgical procedures. High-frequency (50 Hz) ES was applied to the frontal stimulus site (the putative AL) to confirm its language function.
- 4) After tumor resection, we applied 50 Hz ES to the floor of the removal cavity to evaluate the function of the underlying white matter tract. We also applied single-pulse ES to the removal floor and recorded SCEPs from the ventrolateral frontal area and the lateral temporoparietal area. This white matter stimulation was performed in an attempt to trace the language-related tracts into the cortex so that we could evaluate the whole dorsal language pathway.

We describe the actual procedures of the aforementioned methods in the following paragraphs. Intraoperative methods are described first, followed by the preoperative noninvasive methods.

Intraoperative CCEP mapping during general anesthesia

After craniotomy under general anesthesia, strip or grid-type subdural electrodes were placed on the ventrolateral frontal and lateral temporoparietal cortices (see Fig. 1 for electrode configurations). The area of electrode placement was determined according to the noninvasive presurgical fMRI and tractography findings. The electrodes were made of platinum with a recording diameter of 3 mm and an inter-electrode distance of 1 cm (Unique Medical, Tokyo, Japan).

The details of CCEP recording have been reported elsewhere [Matsumoto et al., 2012; Matsumoto et al., 2007; Matsumoto et al., 2004]. A 32-channel intraoperative monitoring system (MEE 1232 Neuromaster, equipped with MS 120B electrical stimulator; Nihon-Kohden, Tokyo, Japan) was used for delivering electric currents and for recording CCEPs and raw electrocorticogram (ECoG). All the data were digitized at a sampling rate of 5000 Hz. To electrically trace the cortico-cortical connections *in vivo*, single-pulse ES was applied to the cortex in a bipolar fashion through a pair of adjacently placed electrodes. Square-wave electrical pulses of alternating polarity with a pulse width of 0.3 ms were delivered at a fixed frequency of 1 Hz and intensity of 10–

15 mA. Recordings from subdural electrodes were referenced to a scalp electrode placed on the skin over the mastoid process contralateral to the side of electrode implantation. CCEPs were online obtained by averaging ECoGs time-locked to the stimulus onset, with a time window of 400 ms (Patient 1, 2, 4, 5, and 6) or 1000 ms (Patient 3), and a band-pass filter of 0.5-1500 Hz (Patient 4–6) or 1-1500 Hz (Patient 1–3). The baseline was set at 4.8 ms (Patient 1, 2, 4, 5, and 6) or 12 ms (Patient 3) before stimulus onset. Two to three trials of 30 responses each were averaged separately to confirm the reproducibility of the responses. During recording, the patients were requested not to perform any tasks, including language tasks, while the patients fully awoke. Raw ECoG was simultaneously recorded to monitor afterdischarges and possible ECoG seizures and to record raw ECoG data for offline analysis.

The candidates for the frontal stimulus site were determined by checking the anatomy carefully [the pars opercularis (IFGop), the pars triangularis (IFGtr) and adjacent areas], the activation area in the fMRI language task, and the cortical terminations of the AF tract drawn by probabilistic diffusion tractography, all of which were implemented in a neuro-navigation system (Vector Vision Compact, BRAINLAB,

Munich, Germany). Three to eight pairs per patient were selected as the candidate stimulus sites. Single-pulse ES was delivered to each candidate site and CCEPs were recorded from the electrodes on the lateral temporoparietal area covering the putative PL. A large CCEP response with an N1 peak at 20–40 ms in the lateral temporoparietal area was considered to represent the cortico-cortical connections between the AL and PL [Matsumoto et al., 2004]. Based on the CCEP distribution, namely, the localization of the maximum CCEP response in the lateral temporoparietal area, the frontal stimulus site was selected for online sequential CCEP recordings. In other words, we determined the putative AL based on the locus of that led to peak CCEP amplitude evoked in PL (i.e., optimal CCEP connectivity pattern).

During the surgical procedure, under general anesthesia, the integrity of the dorsal language pathway was monitored online by stimulating the putative AL and by recording CCEP from the temporoparietal area, i.e., at and around the putative PL, in a sequential fashion at 10- to 15-min of intervals.

Intraoperative CCEP mapping during awake craniotomy

After the patients woke up, during the surgical procedure, language function was evaluated during tumor removal by 1) 1 Hz stimulation to monitor the language network online, i.e., sequential CCEP recording and 2) examining the patient with language batteries: spontaneous speech, reading, picture naming, and word repetition.

In order to confirm language function at the frontal stimulus site, namely, the putative AL, language mapping was performed by conventional 50 Hz cortical ES (square-wave pulse of alternating polarity with a pulse width of 0.3 ms, 3–5 s, 5–12 mA). Reading and picture naming tasks were used. We judged the behaviors as significantly impaired when the findings were reproducible in the absence of afterdischarges [Matsumoto et al., 2011].

Intraoperative SCEP mapping during awake craniotomy

In five out of six patients, after the removal of the tumor, we further evaluated the function and connectivity of the white matter pathway beneath the floor of the removal cavity. In Patient 2, subcortical stimulation was not feasible because of intraoperative brain edema. Strip or grid-type electrodes [1×4 strip (Patient 1, 3, 4, and 6), 2×8 grid

(Patient 5)] were placed so that the stimulus site (a pair of two adjacent electrodes) became the closest to the AF tract integrated in the neuro-navigation. To define the function of the white matter tract, reading and picture naming tasks were performed when high-frequency ES (50 Hz, 3–5 s, 10–15 mA) was applied to the white matter at the stimulus site. Only the impaired behaviors that were reproducible without afterdischarges in ECoG were adopted as significant. To trace the connection from the subcortical stimulus site to the frontal and temporoparietal cortices, single-pulse ES (1 Hz, 10–15 mA, 2×30 trials) were delivered to the stimulus site. SCEPs were recorded from the electrodes on the frontal and temporoparietal cortices. Since a 32-channel intraoperative monitoring system was used, SCEPs and raw ECoG were recorded from the selected electrodes around the frontal stimulus sites and temporoparietal CCEP response sites. The averaging methods of SCEPs were the same as those of CCEPs.

Display and analysis of CCEP and SCEP

As previously reported [Matsumoto et al., 2004], CCEPs consist of an early (N1) negative potential and a late (N2) negative potential. The N1 peak was visually

identified as the first negative deflection that was clearly distinguishable from the stimulus artifacts. The onset, peak latency, and amplitude of N1 were measured as reported previously elsewhere [Matsumoto et al., 2004]. Briefly, a line was drawn from the onset to the offset of the N1 potential for each data point, and the N1 amplitude was measured as the height of a vertical line drawn from the negative peak of N1 to the intersection of the vertical line with the above-described line.

In order to illustrate the distribution of each activity over the cortices, a circle map was employed based on the amplitude percentage distribution, in which the diameter of the circle at each electrode represented the percentile to the maximal amplitude of that particular activity (Fig. 2). Since we had not performed intraoperative MRI, the placement of electrodes was identified based on operative observation and neuro-navigation data.

The CCEP amplitude was continually monitored in comparison with the largest CCEP amplitude recorded at the PL immediately after the patients were awakened. The baseline CCEP amplitude was adopted at this awake condition since general anesthesia could reduce cortical evoked potentials [Howard et al., 2000], and

surgical procedures at and around the language cortex and fibers were usually planned during the awake condition.

In order to avoid intraoperative artifacts, CCEPs and SCEPs were also analyzed offline in MATLAB (Mathworks, Inc., Natick, MA) by averaging ECoGs time-locked to the stimulus onset, with a time window of 600 ms (from 100 ms before to 500 ms after the stimulus onset) and a band-pass filter (the same as intraoperative online methods). The baseline was set at 95 ms before stimulus onset.

MRI data acquisition before and after surgery

MRI scans were performed before and after surgery. Postoperative MRI scans were usually done between 2 and 6 weeks after surgery. Diffusion-weighted images (DWI), fMRI, and a T1 weighted anatomical image were acquired on a 3-Tesla Trio scanner (Siemens, Erlangen, Germany). The parameters of DWI, the T1-weighted image, and the dual gradient field map are reported elsewhere [Oguri et al., 2013]. fMRI was performed only preoperatively by using echo planar imaging (EPI) in an axial orientation with the following parameters: repetition time = 2500 ms, echo time = 30 ms,

flip angle = 90° , voxel size = $3 \times 3 \times 3$ mm, field of view = 192×192 mm, matrix size = 64×64 , 40 slices.

fMRI language task and data analysis

The Japanese shiritori word generation task was used. “Shiritori” is a popular Japanese word chain game to generate an appropriate noun that starts with the last kana letter of the noun presented just before it in tandem. For example, when “ringo” (apple) is presented, the patient must generate a noun beginning with the kana letter “go,” such as “gorira” (gorilla). The activated brain areas are similar to those activated in Western word generation tasks: the left inferior frontal gyrus (IFG) [including IFGop, IFGtr, and the pars orbitalis (IFGor)], the left superior and middle frontal gyri (MFG), the right IFG, and the right cerebellar hemisphere in right-handed healthy subjects [Inoue et al., 2011].

Patients were instructed to do shiritori silently in the activation block and to fixate on a white crosshair, without any body movements, in the rest block following the visual stimuli through a mirror built into the head coil. Each fMRI session consisted

of four activation blocks (30 s each), and five rest blocks (30 s each). Two sessions were performed in each patient.

Functional data were analyzed by FMRIB Software Library (FSL 4.1.6) (FMRIB Centre, Oxford UK) [Smith et al., 2004] and Statistical Parametric Mapping (SPM) 8 (Wellcome Department of Cognitive Neurology, London, UK), as reported elsewhere [Oguri et al., 2013]. Statistical maps comparing the shiritori word generation and rest were calculated at a threshold of $p < 0.001$ (uncorrected).

Diffusion tractography of the AF

The AF was reconstructed by placing two regions of interest (ROI) in the cerebral deep white matter on a coronal directional color-coded map [Matsumoto et al., 2008; Wakana et al., 2007]. To reconstruct the AF tract, an anterior ROI was identified in the coronal slice at the level of the midpoint of the posterior limb of the internal capsule as a triangle-shaped region where the fibers were running in an anterior-posterior orientation. A posterior ROI was identified in the axial slice at the level of the anterior commissure

as a region where the fibers in the superior-inferior orientation were running lateral to the sagittal stratum [Wakana et al., 2007].

Probabilistic diffusion tractography was drawn from the anterior ROI to the posterior ROI by using tools from FSL, as reported elsewhere [Oguri et al., 2013]. To exclude erroneous connections, samples were discarded if they passed into the interhemispheric fissure, thalamus, or ipsilateral peduncle. The threshold of tractography was set to 0.1% of the maximum connectivity value. The connectivity value was the number of samples that pass through the voxel, which was automatically output by the FSL software. This threshold was set lower than in the previous tractography study [Yogarajah et al., 2010], in order to describe the tractography until cortices and to avoid the influence of brain edema caused by the tumor. All the ROI manipulations were performed by one author (Y.Y.) who had sufficient experience with fiber tractography.

Validation of the CCEP/SCEP stimulus and response sites

During the awake condition, language function was confirmed by 50 Hz ES at the stimulus sites for CCEP (the frontal cortex) and SCEP (white matter pathway). In

addition, the anatomical locations of the CCEP/SCEP stimulus and response sites were compared with the activation area of fMRI by the shiritori word generation task and with the cortical terminations of the AF tract. We regarded the findings of the invasive and noninvasive tests as consistent when the distance between the stimulus/response site (either electrode between a pair) and either the activation area of fMRI or the cortical termination of the AF tract was within 7 mm, as reported in a previous combined study of CCEP and tractography [Conner et al., 2011]. As for the CCEP/SCEP response site, the electrodes showing >20% of the amplitude of the maximum response were defined as CCEP/SCEP-positive electrodes, and adopted for validation of the findings of the noninvasive test. We regarded the findings of the AF tract and high-frequency ES in the white matter as consistent when the distance between the AF tract and the stimulus site was within 6 mm, as described in a previous study [Kamada et al., 2007].

Results

CCEP connectivity pattern between the perisylvian language areas

In all patients, single-pulse ES was delivered, under general anesthesia, to the candidate cortices for the frontal stimulus site (3–8 sites per patient), according to the preoperative evaluation. As shown in a representative case (Patient 4, Fig. 3), four candidate stimulus sites were stimulated in the left IFGtr and IFGop, and CCEPs were recorded from the 2 × 8 grid placed in the left temporoparietal area. CCEP connectivity was changed considerably by shifting the stimulus site by 1 cm along the rostrocaudal dimension. It was the stimulation at the IFGtr (the electrode pair of B05-13) that elicited the maximum CCEP response (Electrode A04, N1 peak latency of 25.8 ms) in the posterior part of the STG. The candidate stimulus site that showed the maximum CCEP response in the left lateral temporoparietal area with a relatively early N1 peak was defined as the putative AL. This putative AL was then used as the stimulus site for subsequent online CCEP monitoring. In all patients, the CCEP connectivity pattern successfully delineated the frontal stimulus site (the putative AL) and the maximum CCEP response site (the putative PL) for the sequential monitoring of CCEP amplitude (Fig. 2).

The results of CCEP are summarized in Table 2 and 3. The frontal stimulus site (the electrode pair in the putative AL) was located in the IFGtr in four patients, the

IFGop in three, and the most caudal part of the MFG in one. In all patients, the frontal stimulus site was confirmed as the core AL by high-frequency ES; speech arrest was observed in four patients (Patient 1, 4, 5, and 6), and slowing of speech in two (Patient 2 and 3) during the picture naming task. As expected from the results of high-frequency ES, the location of the frontal stimulus site was consistent with that of fMRI activation in all patients and the cortical terminations of the AF tract in five.

Upon AL stimulation, CCEPs were recorded from the posterior part of the STG (six patients), MTG (four patients), and the inferior temporal gyrus (ITG, three patients) in the temporal lobe, as well as the angular and the supramarginal gyri (AG/SMG, three patients) in the parietal lobe (see Table 3 for N1 latency). In the lateral temporoparietal area, fMRI activation was observed in four patients, and the cortical terminations of the AF tract could be traced into the cortex in all but Patient 2 who had a large tumor and surrounding edema in this area. The distribution of CCEP response sites was consistent with fMRI activation in four patients, and with the cortical terminations of the AF tract in four.

Online CCEP monitoring and functional outcome

Except for two patients in whom the grid was replaced or moved because of clinical necessity when the patients awoke, CCEPs were monitored with the exact same electrode position during both general anesthesia and awake condition (four patients). In these four patients, when the patients woke up, the N1 amplitude increased by an average of 116 μV (ranging from 96 to 139), increased by 60% at the maximum CCEP response site. The CCEP distribution did not change (i.e., did not get wider). As for the N1 latencies, the onset latency changed by an average of 1.0 ms (ranging from -0.8 to 3.3), and the peak latency changed by an average of 0.7 ms (ranging from -0.2 to 1.8).

Waveforms sequentially recorded from a representative case (Patient 3) are shown in Figure 4. The maximum CCEP response was recorded at Electrode B02 on the STG. In this electrode, the N1 amplitude changed from 215 to 311 μV when the patient awoke from general anesthesia. The amplitude did not decline after total removal of the tumor, and she did not have language dysfunction during or after surgery.

In all patients, online CCEP monitoring was sequentially performed in the awake condition. The N1 amplitude at the maximum CCEP response site was compared

with that at the beginning of the awake condition (Fig. 2). In four of six patients, the N1 amplitude did not decrease after tumor resection. In Patient 2, the N1 amplitude decreased from 500 to 440 μV (-12%) after tumor resection. She did not show any language dysfunction during or after surgery. In Patient 4, the N1 amplitude changed from 383 to 260 μV (-32%) after tumor resection (Fig. 2). This patient showed phonemic paraphasia and dyscalculia immediately after waking up. This was most likely due to the partial resection of the left SMG cortex during general anesthesia. No further language deficits developed during tumor removal in the white matter despite the 32% decrease of the N1 amplitude. This patient showed a postoperative decline in the WAB aphasia quotient (80) but she had recovered fully 3 months after surgery (100). In Patient 5, the N1 amplitude of the maximum CCEP response site was 197 and 227 μV before and after tumor resection, respectively (Fig. 2). The N1 amplitude itself did not decline and he did not show any language dysfunction during surgery. The patient, however, developed a decline in verbal fluency, detected by routine neurological examination, immediately after surgery. This temporary symptom might have been caused by postoperative brain edema as judged from MRI findings, and he had

recovered fully 2 months after surgery.

In summary, during tumor resection in the awake condition, CCEP amplitude decreased by 12 or 32% in two patients (Patient 2 and 4). One patient (Patient 4) developed intraoperative language impairment, most likely due to cortical resection, and another patient (Patient 5) developed language impairment immediately after surgery because of brain edema. Language function recovered within a few months in both patients, and none of them had persistent language impairment.

The results of intraoperative monitoring and functional outcome are summarized in Table 3 and partly in Table 1 (WAB scores).

Intraoperative subcortical stimulation

In four of five patients, white matter stimulation (1 Hz) elicited SCEP both at the ventrolateral frontal area (the putative AL) and temporoparietal area (the putative PL) successfully. The results are summarized in Table 4.

Frontal SCEP responses were recorded in the IFGtr in three patients, the IFGop in three, IFGor in three, and the most caudal part of the MFG in three. In all four

patients, the frontal stimulus site for CCEPs was located within the frontal SCEP response sites. The location of the frontal SCEP response site was consistent with that of fMRI activation in all patients and the cortical terminations of the AF tract in three.

Upon stimulation of the white matter, SCEPs were recorded from the STG in four patients, MTG in four, ITG in two, and AG/SMG in one. In all four patients, the temporoparietal site of the maximum CCEP response was located within the temporoparietal SCEP response sites. The distribution of SCEP response sites was consistent with fMRI activation in two patients, and the cortical terminations of the AF tract in two.

In three of five patients (Patient 3–5), high-frequency ES of the white matter produced language impairment in the picture naming task. Arrest of naming was elicited in Patients 3 and 4, and slower naming in Patient 5. The results of white matter functional mapping were consistent with the postoperative tractography study (Supporting Information Fig. 1). Stimulus sites at the floor of removal cavity were close to the AF tract (<6 mm) in three patients (Patient 3–5) who showed naming impairment, while the stimulus site was distant from the AF tract in Patient 1 and 6, who did not.

Waveforms obtained from a representative case (Patient 3) are shown in Figure 5. Circle maps are based on the SCEP amplitude percentage distribution. The largest amplitude SCEP at the putative AL ($SCEP_{WM \rightarrow AL}$) was recorded at Electrode B07 on the IFGtr and that at the putative PL ($SCEP_{WM \rightarrow PL}$) was recorded at Electrode A12 on the MTG. Electrode B07 corresponded with the stimulus site for CCEPs. At Electrode B07, the N1 onset latency of $SCEP_{WM \rightarrow AL}$ was 5.6 ms and the N1 peak latency was 24.6 ms. At Electrode A12, the N1 onset latency of $SCEP_{WM \rightarrow PL}$ was 6.4 ms and the peak latency was 19.6 ms. When the latencies of these two SCEPs, namely, $SCEP_{WM \rightarrow AL}$ and $SCEP_{WM \rightarrow PL}$, were compared with that of $CCEP_{AL \rightarrow PL}$, the sum of SCEP N1 onset latencies (5.6 ms + 6.4 ms = 12.0 ms) approximately corresponded with the onset latency of $CCEP_{AL \rightarrow PL}$ (12.8 ms). The sum of the SCEP N1 peak latencies (44.2 ms) was larger than that of $CCEP_{AL \rightarrow PL}$ (29.2 ms). A similar tendency ($SCEP_{WM \rightarrow AL} + SCEP_{WM \rightarrow PL} \approx CCEP_{AL \rightarrow PL}$) was observed for the onset latencies in Patient 4 and 5, but not in Patient 6 [9.8 ms (sum of SCEPs) vs. 13.0 ms ($CCEP_{AL \rightarrow PL}$)]. In Patient 6, considering that the stimulus site was distant from the AF, evoked potentials elicited by single-pulse ES likely represented cortico-cortical responses from the cortex in the

removal cavity.

Discussion

By applying 50 Hz and single-pulse ES to patients undergoing awake surgery for brain tumors around the AF, we demonstrated that 1) the CCEP connectivity pattern, when combined with preoperative neuroimaging studies, was able to map the anterior and posterior perisylvian language areas, 2) combined (50 Hz and single-pulse) white matter ES delineated both the function and cortical terminations of the “eloquent” language fibers, and 3) intraoperative online CCEP monitoring successfully prevented persistent language impairment in our case series. To the best of our knowledge, we proposed, for the first time, the intraoperative language network monitoring method by employing ES for functional mapping (50 Hz) and tract-tracing (1 Hz).

Subcortical pathway of the dorsal language network

Hickok and Poeppel proposed a dual stream model for language processing [Hickok and Poeppel, 2004]. The dorsal stream engages in auditory-motor integration by mapping

acoustic speech sounds to the articulatory representations, while the ventral stream serves as a sound-to-meaning interface. Recent diffusion tractography studies have revealed that the AF is divided into three components: the anterior, posterior, and long segments. The long segment of the AF connects the IFGop, IFGtr, MFG, and the precentral gyrus to the STG, MTG and ITG, and courses through the parietal lobe without sending projections to the parietal cortex [Catani et al., 2012; Glasser and Rilling, 2008]. The trajectory of the long segment was recently confirmed by a study combining diffusion tractography and postmortem fiber dissection [Martino et al., 2013].

To probe the function of the “language” fibers such as the long segment of the AF, high-frequency ES has been applied to a part of the white matter tract and induced phonemic paraphasia [Kamada et al., 2007; Leclercq et al., 2010]. Even with this gold standard method, we could only obtain evidence that the white matter tract at the stimulus site, i.e., that “one spot” is involved in phonemic processing. We cannot fully argue that this “eloquent spot” constitutes a part of the dorsal language stream.

By applying single-pulse ES to a part of the cortices and by recording CCEPs from the remote cortical regions, we have delineated cortico-cortical networks involved in seizure propagation, as well as various cortical functions, in the extraoperative setting [Enatsu et al., 2013; Matsumoto et al., 2005; Matsumoto et al., 2012; Matsumoto et al., 2007; Matsumoto et al., 2004]. By defining the language cortices using 50 Hz ES, we have demonstrated that the AL and PL are functionally connected with each other [Matsumoto et al., 2004]. In the present intraoperative study, we employed white matter 50 Hz and single-pulse ES in an attempt to obtain evidence that the “eloquent spot” connects to both the AL and PL, thereby constituting a part of the eloquent language pathways. In three patients (Patient 3–5), we were able to functionally map the “eloquent spot” at or close to the AF (within 6 mm) by 50 Hz ES. By recording SCEPs, single-pulse ES successfully traced the connections from the stimulus site, i.e., the eloquent spot, into the AL and PL as defined by noninvasive (fMRI, tractography) and invasive (50 Hz ES) findings. In summary, the present combined cortical- and subcortical ES study, provided the direct evidence, for the first time, that the AL, PL, and AF (long segment) constitute the dorsal language network. The present findings

support a previous noninvasive study in healthy subjects that traced the AF tract between the frontal and temporal areas activated during sublexical repetition of speech to propose the existence of a dorsal language route for sensorimotor mapping of sound to articulation [Saur et al., 2008]. We failed to produce phonemic paraphasia during white matter high-frequency ES probably because we used relatively high intensity of electric current (10–15 mA). Stimulation at higher intensity in this pilot study as compared with previous studies [Duffau et al., 2005; Kamada et al., 2007; Maldonado et al., 2011] likely resulted in the arrest or slowing of naming. High-frequency white matter ES at a lower intensity may be warranted for functional characterization of the dorsal language pathway in future investigations.

Implication of CCEP and SCEP

In extraoperative settings, CCEP has been extensively employed to investigate functional cortical networks and seizure propagation tracts [Catenoix et al., 2005; Catenoix et al., 2011; Keller et al., 2011; Koubeissi et al., 2012; Kubota et al., 2013; Lacruz et al., 2007; Matsumoto et al., 2004; Matsuzaki et al., 2013; Rosenberg et al.,

2009]. It has been effective in locating inter-connected cortical regions, but its precise generator mechanism still remains unclear. Two possible modes of impulse propagation have been proposed: direct cortico-cortical propagation through white matter tracts, and indirect cortico-subcortico-cortical propagation via subcortical structures. Our recent parietofrontal connectivity study showed a linear correlation between the N1 peak latency and the surface distance from the parietal stimulus site to the frontal response site [Matsumoto et al., 2012]. This observation favors the direct cortico-cortical white matter pathway, because the longer the surface distance is, the proportionally longer the actual white matter pathway connecting the two cortical sites and, accordingly, its traveling time, is. Indeed, short latency CCEPs were recorded from the parietal depth electrodes in the superior longitudinal fasciculus by single pulse ES of the premotor area in another study [Enatsu et al., 2013]. In the present study, a comparison between SCEP and CCEP latencies provided further insight into the mode of impulse propagation. In three patients (Patient 3–5) in whom we successfully traced the connections from the AF to the cortical language areas by SCEPs, it was the sum of SCEP N1 onset latencies that approximately corresponded with the onset latency of

CCEP_{AL→PL}. The N1 onset or the first positive deflection is proposed to represent the fastest monosynaptic impulse projecting into the middle or deep cortical layers via large cortico-cortical projection fibers, giving rise to a small positive surface potential [Felleman and Van Essen, 1991; Terada et al., 2012]. If this is the case, our findings support the hypothesis that the impulse is conveyed directly through the white matter pathways. On the other hand, the sum of the SCEP N1 peak latencies was longer than CCEP_{AL→PL} N1 peak latency. The CCEP N1 peak likely represents the summation of direct cortico-cortical impulses conveyed both by small fibers with slower conduction velocities and by large myelinated fibers activated through indirect oligo-synaptic cortico-cortical projections. In this sense, as in intraoperative MEP monitoring, it is plausible to use the N1 amplitude as a surrogate marker of the integrity of the white matter tract.

Clinical relevance of intraoperative language network monitoring

Under general anesthesia, single-pulse ES was applied to several candidate cortical locations for the frontal stimulus site (the putative AL) according to the noninvasive

anatomical (gyral patterns) and functional (fMRI) findings. By comparing CCEP distribution with the anatomy (terminations of the AF tract) and function (fMRI) in the lateral temporoparietal area, the frontal stimulus site, namely, the putative AL, was determined in each patient. Of note, the CCEP connectivity pattern successfully localized the frontal stimulus site at the core AL where high-frequency ES produced language impairment in all patients. Functional cortical mapping with high-frequency ES is regarded as one of the gold standard methods for mapping language areas during awake craniotomy, but it may induce seizures. In the present pilot study, the fMRI shiritori word generation task located the AL (100%) and PL in all but two patients (66%). When we could adopt other language tasks, such as reading or listening, that activates the PL in a more efficient way by using fMRI or magnetoencephalography [Kamada et al., 2007; Saur et al., 2008], the CCEP connectivity pattern, together with preoperative tractography and functional mapping, could probe the interconnected AL and PL without high-frequency ES in individual patients. It should be noted that a wide craniotomy was needed for intraoperative language network monitoring in order to place subdural electrodes to the perisylvian language areas as is the case with

subcortical or cortical high frequency ES studies to identify language function [Berger et al., 1989; Kamada et al., 2007; Maldonado et al., 2011].

After defining the frontal stimulus site with the CCEP connectivity pattern, the integrity of the dorsal language pathway was monitored online by stimulating the AL and recording CCEPs from the temporoparietal area in a sequential manner. Online sequential CCEP monitoring was feasible during awake craniotomy, because of the high reproducibility and reliability of CCEP waveforms (amplitude, latency). Moreover, intraoperative CCEP monitoring was performed safely, without provoking any adverse events such as seizures during surgical procedures in all patients. A decrease of CCEP amplitude by less than 32% did not produce persistent language impairment in our case series. However, our pilot study could not yield a clear cut-off value due to a limited number of participants. By analogy to MEP [Macdonald, 2006], 50% might be an appropriate cut-off value, but further case accumulation is warranted for establishing the sensitivity and specificity of this method for its clinical usefulness.

In Patient 2, brain edema surrounding the tumor was too extensive to trace the AF tract into the posterior temporal area, even by probabilistic diffusion tractography.

Despite brain edema, CCEP was recorded from the STG and MTG where the PL was indicated by the fMRI shiritori word generation task. The discrepancy in the positive rate between the fMRI language task and tractography is well documented in patients with brain tumors. Bizzi et al. [Bizzi et al., 2012] reported that in 19 patients with glioma in the ventrolateral frontal region, the IFGop was identified with fMRI (verb generation task) in 17 patients (95%), while the AF was detected only in five patients (26%), dislocated in eight patients, and interrupted in six patients. In Patient 2, although the CCEP amplitude decreased by 12%, language function was preserved during and after surgery. The integrity of the subcortical language pathway could be monitored intraoperatively by CCEPs even when diffusion tractography failed to trace the AF tract beyond the region of brain edema.

Because of possible brain shift during awake craniotomy, the exact relationship between the site of subcortical ES and the AF was evaluated by postoperative MRI. The stimulus sites corresponded with the AF in three of five patients (60%). The concordance rate was similar to the one reported in a previous study combining subcortical high-frequency ES and diffusion tensor tractography [Ellmore et

al., 2009]. The discordance usually resulted in negative findings as in Patient 1.

Alternatively, stimulation of other language-related tracts [Ellmore et al., 2009] or that of the sulcal part of the cortex at the floor of removal cavity might lead to false positive findings, e.g., language impairment or SCEP responses whose latencies did not fit $CCEP_{AL-PL}$ latency as in Patient 6. Combined 50 Hz and single-pulse subcortical ES would complement diffusion tractography and help clarify the site of stimulation for intraoperative language mapping.

Kokkinos et al. [Kokkinos et al., 2013] reported that delayed responses evoked by single-pulse ES showed similar topography between general anesthesia and awake condition. In the present study, although the amplitudes were less than those recorded in the awake condition, CCEPs were well recorded under general anesthesia and the CCEP connectivity pattern could localize the AL and PL in all patients. In patients in whom electrode location did not change throughout surgery, the CCEP distribution did not change (i.e., did not get larger) in the awake condition. When combined with noninvasive functional and anatomical neuroimaging techniques, intraoperative language network mapping under general anesthesia would be promising

for preservation of the dorsal language network. Comparing the findings under general anesthesia with those during the awake condition in a larger number of patients is warranted to establish its clinical utility. Moreover, a similar intraoperative network mapping would be applicable for the ventral language pathway involved in language comprehension. The target white matter pathways for this network would be either the inferior longitudinal fasciculus or the inferior fronto-occipital fasciculus, since 50 Hz white matter ES elicited semantic paraphasia [Duffau et al., 2005; Mandonnet et al., 2007]. To this end, combined 50 Hz and single-pulse ES should be applied first during awake craniotomy to probe the cortical and white matter function and their connections.

Acknowledgements

We are indebted to Dr. Masato Hojo for providing the patients' data. This work was partly supported by Grants-in-Aid for Scientific Research (C) 24592159 (TK), 23591273 (RM), from the Ministry of Education, Culture, Sports, Science and Technology of Japan, and the Research Grant from Takeda Science Foundation.

References

Behrens TE, Berg HJ, Jbabdi S, Rushworth MF, Woolrich MW (2007): Probabilistic diffusion tractography with multiple fibre orientations: What can we gain?

NeuroImage 34:144-55.

Berger MS, Kincaid J, Ojemann GA, Lettich E (1989): Brain mapping techniques to maximize resection, safety, and seizure control in children with brain tumors.

Neurosurgery 25:786-92.

Bizzi A, Nava S, Ferre F, Castelli G, Aquino D, Ciaraffa F, Broggi G, DiMeco F,

Piacentini S (2012): Aphasia induced by gliomas growing in the ventrolateral

frontal region: assessment with diffusion MR tractography, functional MR

imaging and neuropsychology. Cortex 48:255-72.

Catani M, Dell'acqua F, Bizzi A, Forkel SJ, Williams SC, Simmons A, Murphy DG,

Thiebaut de Schotten M (2012): Beyond cortical localization in

clinico-anatomical correlation. Cortex 48:1262-87.

Catenoix H, Magnin M, Guenot M, Isnard J, Manguiere F, Ryvlin P (2005):

Hippocampal-orbitofrontal connectivity in human: an electrical stimulation

study. *Clin Neurophysiol* 116:1779-84.

Catenoix H, Magnin M, Mauguiere F, Ryvlin P (2011): Evoked potential study of hippocampal efferent projections in the human brain. *Clin Neurophysiol* 122:2488-97.

Conner CR, Ellmore TM, DiSano MA, Pieters TA, Potter AW, Tandon N (2011): Anatomic and electro-physiologic connectivity of the language system: a combined DTI-CCEP study. *Comput Biol Med* 41:1100-9.

Duffau H (2008): The anatomo-functional connectivity of language revisited. New insights provided by electrostimulation and tractography. *Neuropsychologia* 46:927-34.

Duffau H, Gatignol P, Mandonnet E, Peruzzi P, Tzourio-Mazoyer N, Capelle L (2005): New insights into the anatomo-functional connectivity of the semantic system: a study using cortico-subcortical electrostimulations. *Brain* 128:797-810.

Ellmore TM, Beauchamp MS, O'Neill TJ, Dreyer S, Tandon N (2009): Relationships between essential cortical language sites and subcortical pathways. *J Neurosurg* 111:755-66.

Enatsu R, Matsumoto R, Piao Z, O'Connor T, Horning K, Burgess RC, Bulacio J,

Bingaman W, Nair DR (2013): Cortical negative motor network in comparison with sensorimotor network: a cortico-cortical evoked potential study. *Cortex* 49:2080-96.

Felleman DJ, Van Essen DC (1991): Distributed hierarchical processing in the primate cerebral cortex. *Cereb Cortex* 1:1-47.

Glasser MF, Rilling JK (2008): DTI tractography of the human brain's language pathways. *Cereb Cortex* 18:2471-82.

Hickok G, Poeppel D (2004): Dorsal and ventral streams: a framework for understanding aspects of the functional anatomy of language. *Cognition* 92:67-99.

Howard MA, Volkov IO, Mirsky R, Garell PC, Noh MD, Granner M, Damasio H, Steinschneider M, Reale RA, Hind JE, Brugge JF (2000): Auditory cortex on the human posterior superior temporal gyrus. *J Comp Neurol* 416:79-92.

Inoue M, Ueno T, Morita K, Shoji Y, Matsuoka T, Fujiki R, Abe T, Uchimura N (2011): Brain activities on fMRI using the shiritori task in normal subjects.

Kurume Med J 57:109-15.

July J, Manninen P, Lai J, Yao Z, Bernstein M (2009): The history of awake craniotomy for brain tumor and its spread into Asia. Surg Neurol 71:621-4; discussion 624-5.

Kamada K, Todo T, Masutani Y, Aoki S, Ino K, Morita A, Saito N (2007):

Visualization of the frontotemporal language fibers by tractography combined with functional magnetic resonance imaging and magnetoencephalography. J Neurosurg 106:90-8.

Keller CJ, Bickel S, Entz L, Ulbert I, Milham MP, Kelly C, Mehta AD (2011): Intrinsic functional architecture predicts electrically evoked responses in the human brain. Proc Natl Acad Sci U S A 108:10308-13.

Kokkinos V, Alarcon G, Selway RP, Valentin A (2013): Role of single pulse electrical stimulation (SPES) to guide electrode implantation under general anaesthesia in presurgical assessment of epilepsy. Seizure 22:198-204.

Koubeissi MZ, Lesser RP, Sinai A, Gaillard WD, Franaszczuk PJ, Crone NE (2012):

Connectivity between perisylvian and bilateral basal temporal cortices. Cereb

Cortex 22:918-25.

Kubota Y, Enatsu R, Gonzalez-Martinez J, Bulacio J, Mosher J, Burgess RC, Nair DR

(2013): In vivo human hippocampal cingulate connectivity: A corticocortical evoked potentials (CCEPs) study. Clin Neurophysiol 124:1547-56.

Lacruz ME, Garcia Seoane JJ, Valentin A, Selway R, Alarcon G (2007): Frontal and

temporal functional connections of the living human brain. Eur J Neurosci 26:1357-70.

Leclercq D, Duffau H, Delmaire C, Capelle L, Gatignol P, Ducros M, Chiras J,

Lehericy S (2010): Comparison of diffusion tensor imaging tractography of language tracts and intraoperative subcortical stimulations. J Neurosurg 112:503-11.

Macdonald DB (2006): Intraoperative motor evoked potential monitoring: overview and

update. J Clin Monit Comput 20:347-77.

Maldonado IL, Moritz-Gasser S, Duffau H (2011): Does the left superior longitudinal

fascicle subserve language semantics? A brain electrostimulation study. Brain Struct Funct 216:263-74.

Mandonnet E, Nouet A, Gatignol P, Capelle L, Duffau H (2007): Does the left inferior longitudinal fasciculus play a role in language? A brain stimulation study. *Brain* 130:623-9.

Martino J, De Witt Hamer PC, Berger MS, Lawton MT, Arnold CM, de Lucas EM, Duffau H (2013): Analysis of the subcomponents and cortical terminations of the perisylvian superior longitudinal fasciculus: a fiber dissection and DTI tractography study. *Brain Struct Funct* 218:105-21.

Matsumoto R, Imamura H, Inouchi M, Nakagawa T, Yokoyama Y, Matsushashi M, Mikuni N, Miyamoto S, Fukuyama H, Takahashi R, Ikeda A (2011): Left anterior temporal cortex actively engages in speech perception: A direct cortical stimulation study. *Neuropsychologia* 49:1350-4.

Matsumoto R, Kinoshita M, Taki J, Hitomi T, Mikuni N, Shibasaki H, Fukuyama H, Hashimoto N, Ikeda A (2005): In vivo epileptogenicity of focal cortical dysplasia: a direct cortical paired stimulation study. *Epilepsia* 46:1744-9.

Matsumoto R, Nair DR, Ikeda A, Fumuro T, Lapresto E, Mikuni N, Bingaman W, Miyamoto S, Fukuyama H, Takahashi R, Najm I, Shibasaki H, Luders HO

(2012): Parieto-frontal network in humans studied by cortico-cortical evoked potential. *Hum Brain Mapp* 33:2856-72.

Matsumoto R, Nair DR, LaPresto E, Bingaman W, Shibasaki H, Luders HO (2007):

Functional connectivity in human cortical motor system: a cortico-cortical evoked potential study. *Brain* 130:181-97.

Matsumoto R, Nair DR, LaPresto E, Najm I, Bingaman W, Shibasaki H, Luders HO

(2004): Functional connectivity in the human language system: a cortico-cortical evoked potential study. *Brain* 127:2316-30.

Matsumoto R, Okada T, Mikuni N, Mitsueda-Ono T, Taki J, Sawamoto N, Hanakawa T,

Miki Y, Hashimoto N, Fukuyama H, Takahashi R, Ikeda A (2008): Hemispheric asymmetry of the arcuate fasciculus. *Journal of Neurology* 255:1703-1711.

Matsuzaki N, Juhász C, Asano E (2013): Cortico-cortical evoked potentials and

stimulation-elicited gamma activity preferentially propagate from lower- to higher-order visual areas. *Clin Neurophysiol* 124:1290-6.

Mori S, van Zijl PC (2002): Fiber tracking: principles and strategies - a technical review.

NMR Biomed 15:468-80.

Oguri T, Sawamoto N, Tabu H, Urayama S, Matsushashi M, Matsukawa N, Ojika K,

Fukuyama H (2013): Overlapping connections within the motor cortico-basal ganglia circuit: fMRI-tractography analysis. *NeuroImage* 78:353-62.

Rosenberg DS, Mauguiere F, Catenoux H, Faillenot I, Magnin M (2009): Reciprocal

thalamocortical connectivity of the medial pulvinar: a depth stimulation and evoked potential study in human brain. *Cereb Cortex* 19:1462-73.

Saur D, Kreher BW, Schnell S, Kummerer D, Kellmeyer P, Vry MS, Umarova R,

Musso M, Glauche V, Abel S, Huber W, Rijntjes M, Hennig J, Weiller C

(2008): Ventral and dorsal pathways for language. *Proc Natl Acad Sci U S A* 105:18035-40.

Silbergeld DL, Mueller WM, Colley PS, Ojemann GA, Lettich E (1992): Use of

propofol (Diprivan) for awake craniotomies: technical note. *Surg Neurol* 38:271-2.

Smith SM, Jenkinson M, Woolrich MW, Beckmann CF, Behrens TE, Johansen-Berg H,

Bannister PR, De Luca M, Drobnjak I, Flitney DE, Niazy RK, Saunders J,

Vickers J, Zhang Y, De Stefano N, Brady JM, Matthews PM (2004): Advances

in functional and structural MR image analysis and implementation as FSL.

NeuroImage 23 Suppl 1:S208-19.

Takayama M, Miyamoto S, Ikeda A, Mikuni N, Takahashi JB, Usui K, Satow T,

Yamamoto J, Matsushashi M, Matsumoto R, Nagamine T, Shibasaki H,

Hashimoto N (2004): Intracarotid propofol test for speech and memory

dominance in man. Neurology 63:510-5.

Terada K, Umeoka S, Usui N, Baba K, Usui K, Fujitani S, Matsuda K, Tottori T,

Nakamura F, Inoue Y (2012): Uneven interhemispheric connections between

left and right primary sensori-motor areas. Hum Brain Mapp 33:14-26.

Wakana S, Caprihan A, Panzenboeck MM, Fallon JH, Perry M, Gollub RL, Hua K,

Zhang J, Jiang H, Dubey P, Blitz A, van Zijl P, Mori S (2007): Reproducibility

of quantitative tractography methods applied to cerebral white matter.

NeuroImage 36:630-44.

Whitaker HA, Ojemann GA (1977): Graded localisation of naming from electrical

stimulation mapping of left cerebral cortex. Nature 270:50-1.

Yogarajah M, Focke NK, Bonelli SB, Thompson P, Vollmar C, McEvoy AW,

Alexander DC, Symms MR, Koepp MJ, Duncan JS (2010): The structural plasticity of white matter networks following anterior temporal lobe resection.

Brain 133:2348-64.

Figure Legend**Figure 1**

Noninvasive anatomic-functional mapping of the dorsal language network. The left column: 3D MRI shows the long segment of the arcuate fasciculus (AF) (green) and the tumor (red) around the AF. The middle column: The anterior and posterior perisylvian language cortices defined by shiritori word generation fMRI (dark yellow) are shown in comparison with the subdural electrodes. Only the activation areas outside the pre- and postcentral gyri are shown for clarity. White circles denote visible electrodes in the operative view, and gray circles invisible electrodes. Note that the frontal CCEP stimulus site (a black pair of electrodes) corresponded with the anterior language area defined by fMRI in all patients. The right column: The AF tracts (green) were shown in comparison with subdural electrodes.

Figure 2

Behavior of the CCEP N1 amplitude during tumor removal in the awake condition. The left column shows the CCEP distribution with a circle map in each patient in the awake condition. The diameter of the circle at each electrode represented the percentile to the largest amplitude at the maximum CCEP response site. The right column shows the N1 waveform at the maximum CCEP response site in each patient. The black line represents the N1 waveform immediately after the awake condition, and the red line that after tumor removal. A N1 amplitude decrease was noted in Patient 2 (12%) and Patient 4 (32%).

Figure 3

CCEP connectivity pattern to map perisylvian language areas (Patient 4). Under general anesthesia, single-pulse electrical stimulation was delivered to four candidate sites (Plate B) according to the noninvasive anatomic-functional mapping, and CCEPs were recorded from the temporoparietal area (Plate A). Two trials are plotted in superimposition at each electrode. The vertical bar corresponds to the time of stimulation. Note the CCEP pattern in Plate A differs evidently among the four stimulus

sites. Electrode B05-13 stimulation showed the largest and most discrete CCEP response in the lateral temporoparietal area (Electrode A04 and A05). This site was regarded as the putative anterior language area. Indeed 50 Hz stimulation of this area showed language impairment in the awake condition. n.a. = CCEP was not available due to high impedance in the recording electrode. Other conventions are the same as for Figure 1.

Figure 4

Intraoperative online language network mapping by CCEPs (Patient 3). A. Electrode configuration in the intraoperative view. B. CCEP distribution map during general anesthesia. CCEP distributed over the middle to posterior part of the superior, middle and inferior temporal gyri (the maximum at Electrode B02 in the superior temporal gyrus). C. CCEP waveforms (Plate B) in the awake condition (before tumor removal). Two trials are plotted in superimposition. CCEP distribution did not change between general anesthesia and awake condition. D. Change of the N1 amplitude during surgery at the maximum CCEP response site (Electrode B02). CCEP waveforms are

sequentially shown from the top to the bottom along the time course of surgery. As the patient awoke, the N1 amplitude increased from 215 to 311 μV (+45%). After tumor removal the N1 amplitude did not decline (329 μV). She did not show language dysfunction during or after surgery. Other conventions are the same as for Figure 3.

Figure 5

Subcortico-cortical evoked potentials (SCEPs) in Patient 3.

A. Site of white matter stimulation. Electrode pair (highlighted by a green circle) was stimulated at the floor of the removal cavity (right). The stimulus site (cross hairs) was attached to the arcuate fasciculus (long segment) in the neuro-navigation (left).

High-frequency (50 Hz) stimulation at this site induced the arrest of naming. B. SCEP

distribution in the frontal and temporal areas. Circle maps were made separately for

SCEP responses in the frontal ($\text{SCEP}_{\text{WM} \rightarrow \text{AL}}$) and temporal ($\text{SCEP}_{\text{WM} \rightarrow \text{PL}}$) areas, based

on the SCEP amplitude percentage distribution. C. $\text{SCEP}_{\text{WM} \rightarrow \text{AL}}$ (Plate B) and

$\text{SCEP}_{\text{WM} \rightarrow \text{PL}}$ (Plate A) waveforms. The largest response was highlighted with a dotted

circle and its onset and peak latencies are shown in the enlarged waveform at the bottom.

n.a. = SCEP was not available due to the limited number of channels available for simultaneous monitoring or high impedance in the recording electrode. Other conventions are the same as for Figure 4.

Supporting Information Figure 1

Relationship between the arcuate fasciculus (green, long segment) and the stimulus site for white matter stimulation. The arcuate fasciculus (long segment) was traced by diffusion tractography using MRI data performed after the operation. Five patients in whom both 50 Hz and single-pulse stimulation was applied to the white matter at the floor of the removal cavity are shown. The distance between the stimulus site and the arcuate fasciculus was shown on the left to 2D MRI images.

Table 1 Patient demographics

	Age	Gender	Tumor location	Language dominance	Preoperative symptoms	Tumor pathology	WAB aphasia quotient		
							before surgery	after surgery	
								2-6 weeks	3 months
Patient 1	28	male	Ins, STG	left	seizure, right hemiparesis	anaplastic astrocytoma	99.9	99.6	n.a.
Patient 2	31	female	Ins, STG, MTG	left	cognitive impairment, quadrantanopsia	WHO grade II-III astrocytoma	nl*	95.6	n.a.
Patient 3	19	female	AG, SMG, PoCG	left	seizure	DNT	100	100	n.a.
Patient 4	44	female	AG, SMG, PoCG	left	seizure	diffuse astrocytoma	99.5	80	100
Patient 5	38	male	IFG	left	seizure	oligodendroglioma	97.7	68.3	93
Patient 6	36	female	SMG	left	asymptomatic	DNT	100	100	n.a.

Ins = insula; MTG = middle temporal gyrus; PoCG = postcentral gyrus; SMG = supramarginal gyrus; AG = angular gyrus; STG = superior temporal gyrus; IFG = inferior frontal gyrus; DNT = dysembryoplastic neuroepithelial tumor; n.a. = not available

* normal language function by clinical examination

Table 2 CCEP connectivity pattern

	frontal stimulus sites (location of electrode pair)			CCEP _{AL→PL} response				Consistency with fMRI (language cortex)		Consistency with diffusion tractography (the AF tract)	
	IFGtr	IFGop	MFG	STG	MTG	ITG	AG / SMG	AL	PL	AL	PL
Patient 1	+			+		+	++	Yes	Yes	Yes	Yes
Patient 2	+	+		+	++		+	Yes	Yes	Yes	No
Patient 3	+	+		++	+	+		Yes	Yes	Yes	Yes
Patient 4	+			++	+			Yes	n.a.	Yes	Yes
Patient 5			+	++			+	Yes	n.a.	Yes	No
Patient 6	+	+		+	+	++		Yes	Yes	No	Yes

IFGtr = inferior frontal gyrus pars triangularis; IFGop = inferior frontal gyrus pars opercularis; MFG = middle frontal gyrus; STG = superior temporal gyrus; MTG = middle temporal gyrus; ITG = inferior temporal gyrus; AG = angular gyrus; SMG = supramarginal gyrus; AF = arcuate fasciculus; AL = anterior language area; PL = posterior language area; n.a. = not available (no fMRI activation); ++ the largest CCEP response

Table 3 Intraoperative language network mapping and functional outcome

	Cortical HFES at the frontal stimulus site	CCEP _{AL→PL} N1 latency (ms)		CCEP amplitude decrease (%)	Subcortical HFES at WM stimulus site	SCEP N1 latency (ms)					Language disturbance	
		Language impairment	onset			peak	Language impairment	SCEP _{WM→AL}		SCEP _{WM→PL}		SCEP _{WM→AL} + SCEP _{WM→PL}
	onset			peak	onset			peak	onset / peak			
Patient 1	Yes	7.6	30.8	0	No	no response					No	No
Patient 2	Yes	12.8	27.4	12	n.a.	n.a.	n.a.	n.a.	n.a.	n.a.	No	No
Patient 3	Yes	12.8	29.2	0	Yes	5.6	24.6	6.4	19.6	12.0 / 44.2	No	No
Patient 4	Yes	11.0	25.0	32	Yes	7.2	19.0	4.2	12.0	11.4 / 31.0	Yes*	Yes
Patient 5	Yes	9.6	32.0	0	Yes	6.2	17.6	4.0	15.8	10.2 / 33.4	No	Yes
Patient 6	Yes	13.0	33.2	0	No	6.6	22.6	3.2	18.0	9.8 / 40.6	No	No

All latencies were measured in the awake condition.

HFES = high-frequency electrical stimulation; AL = anterior language area; PL = posterior language area; WM = white matter; n.a. = not available (no stimulation); * Language disturbance was already observed before the CCEP amplitude decreased because of the partial cortical resection of the supramarginal gyrus

Table 4 SCEP connectivity pattern

	SCEP _{WM→AL} response				SCEP _{WM→PL} response				Consistency with fMRI (language cortex)		Consistency with diffusion tractography (the AF tract)	
	IFGor	IFGtr	IFGop	MFG	STG	MTG	ITG	AG / SMG	AL	PL	AL	PL
Patient 3	+	+	++	+	+	+	++		Yes	Yes	Yes	Yes
Patient 4	+	++	+	+	+	++			Yes	n.a.	Yes	Yes
Patient 5				++	+	++		+	Yes	n.a.	Yes	No
Patient 6	+	+	++		++	+	+		Yes	Yes	No	No

Only patients in whom SCEP was recorded successfully are shown.

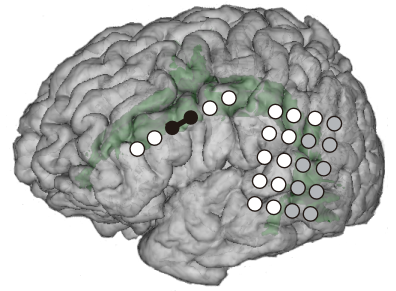
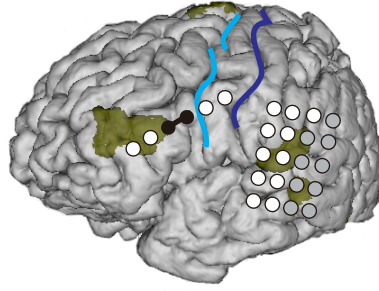
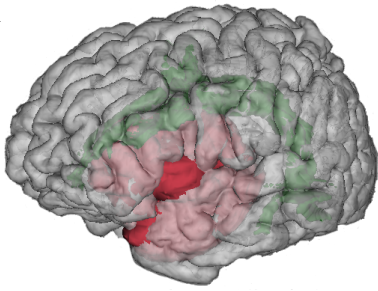
IFGtr = inferior frontal gyrus pars orbitalis; IFGtr = inferior frontal gyrus pars triangularis; IFGop = inferior frontal gyrus pars opecularis; MFG = middle frontal gyrus; STG = superior temporal gyrus; MTG = middle temporal gyrus; ITG = inferior temporal gyrus; AG = angular gyrus; SMG = supramarginal gyrus; AF = arcuate fasciculus; AL = anterior language area; PL = posterior language area; WM = white matter; n.a. = not available (no fMRI activation) ; ++ the largest SCEP response

tumor

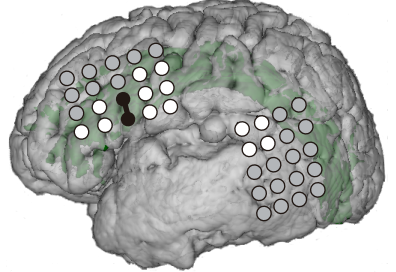
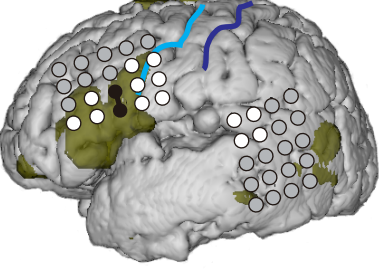
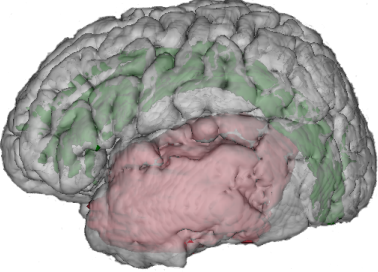
language fMRI

arcuate fasciculus
(long segment)

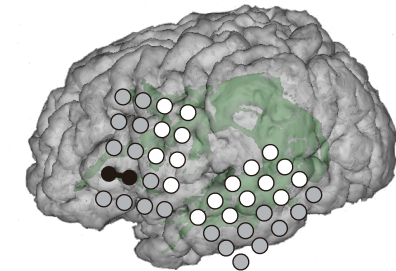
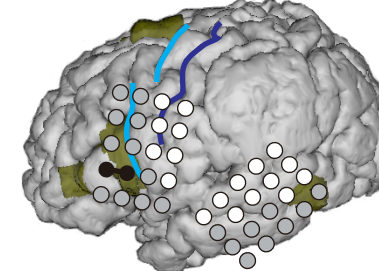
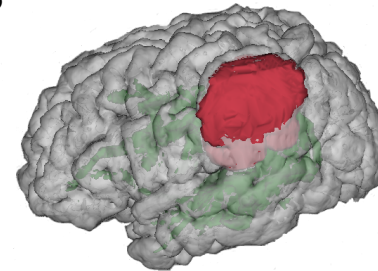
Patient 1



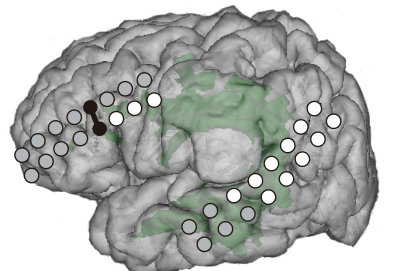
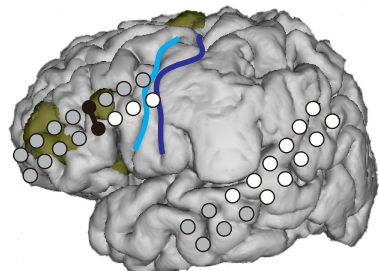
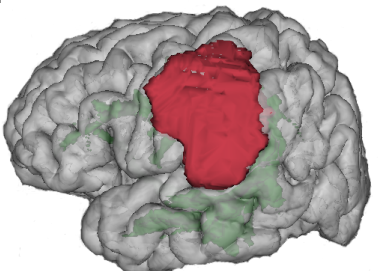
Patient 2



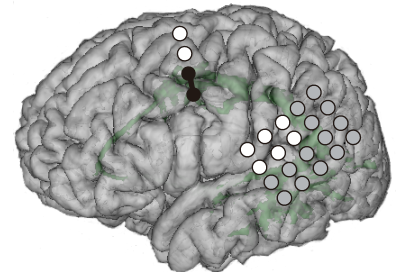
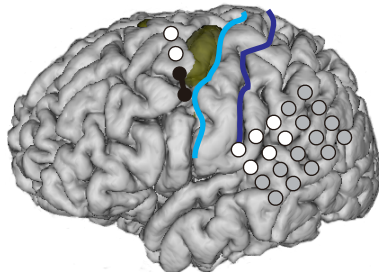
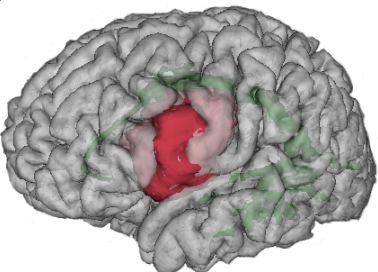
Patient 3



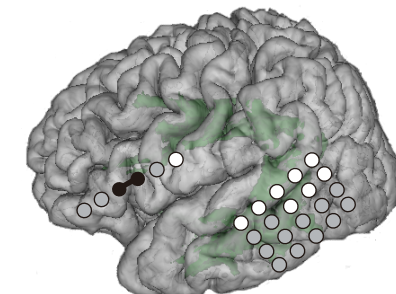
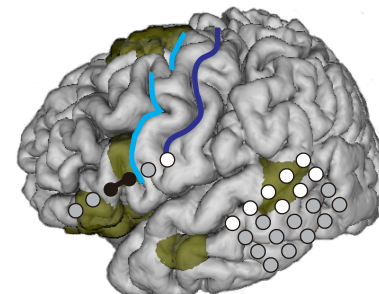
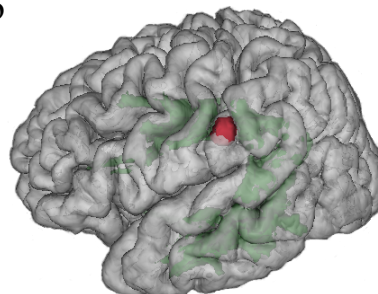
Patient 4



Patient 5



Patient 6



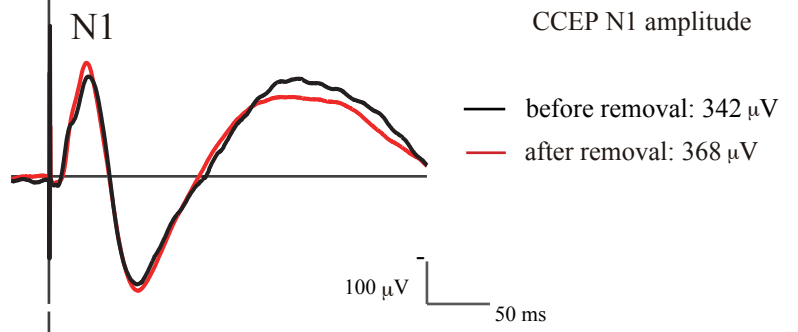
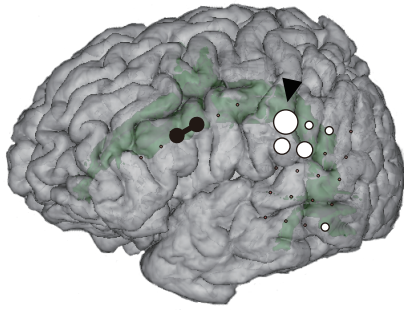
- visible electrode
- invisible electrode
- stimulus site

- tumor
- arcuate fasciculus
- fMRI activation

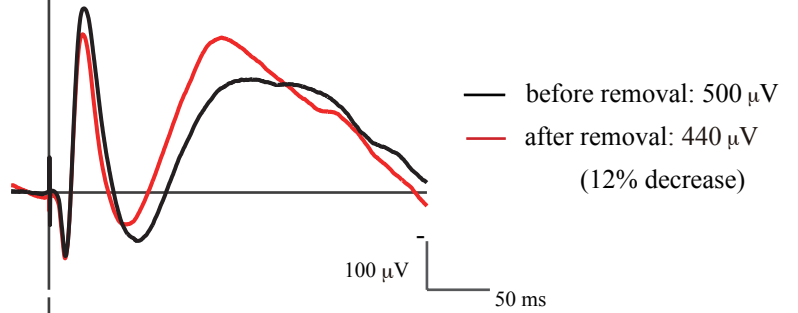
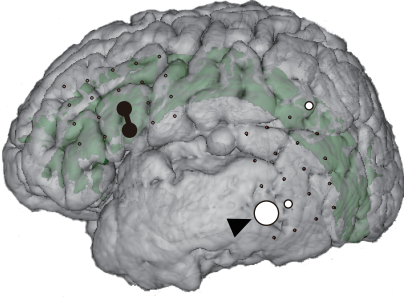
- central sulcus
- precentral sulcus

CCEP waveform at the maximum response site
before and after removal

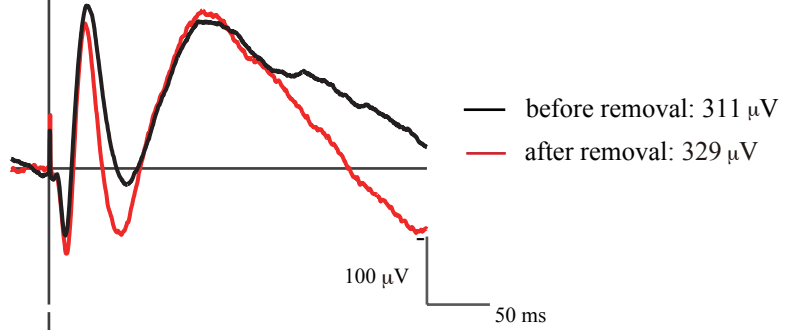
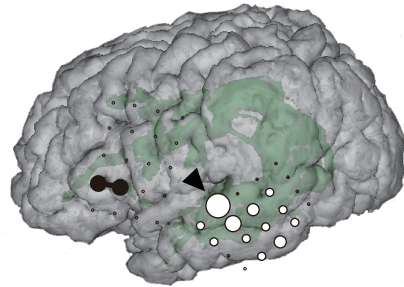
Patient 1



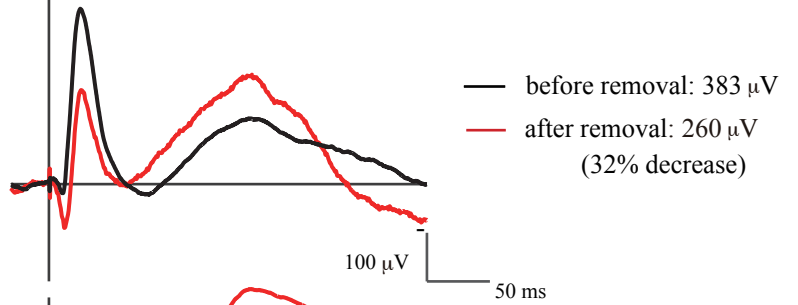
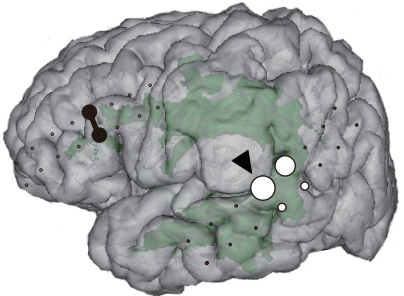
Patient 2



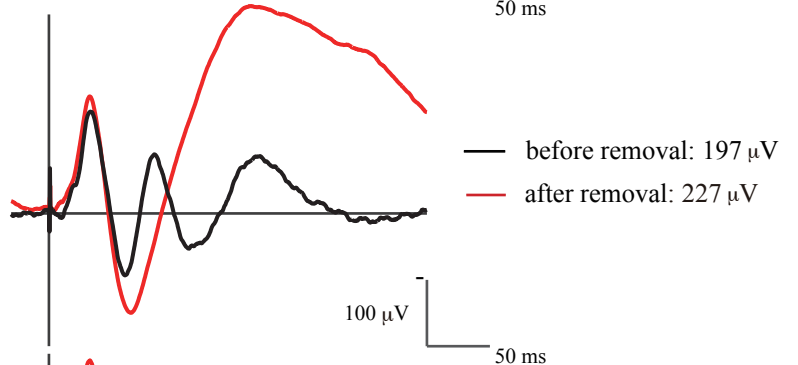
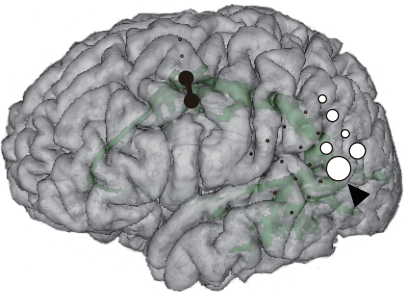
Patient 3



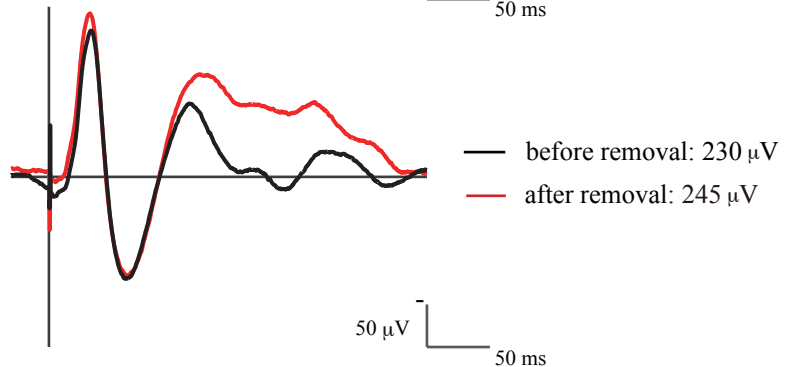
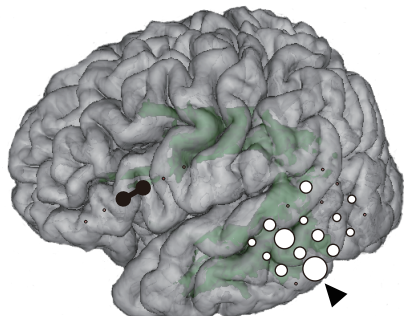
Patient 4



Patient 5



Patient 6



N1 amplitude

- 100%
- 80%-
- 60%-
- 40%-
- 20%-

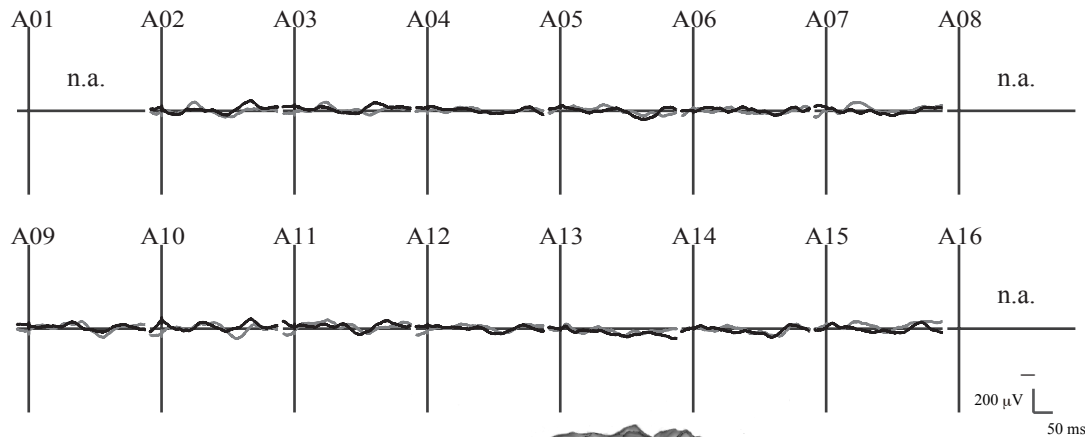
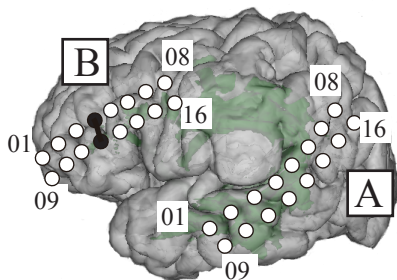
● stimulus site

○ CCEP response site

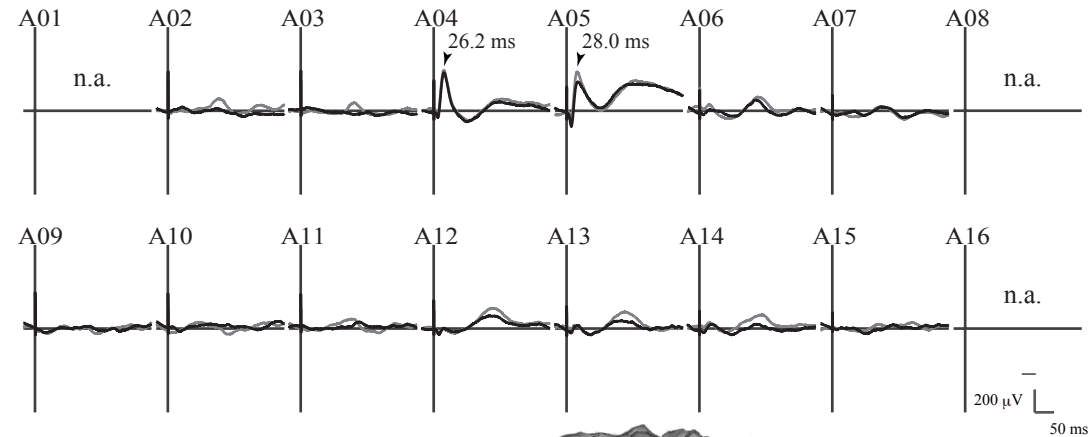
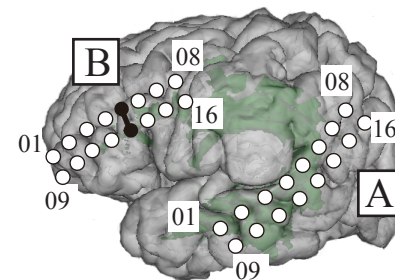
▶ the maximum CCEP response site

➤ arcuate fasciculus

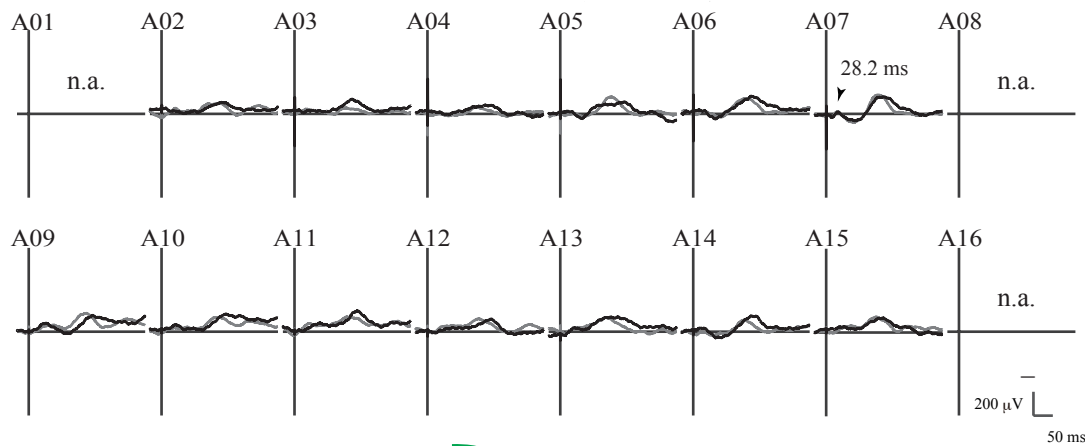
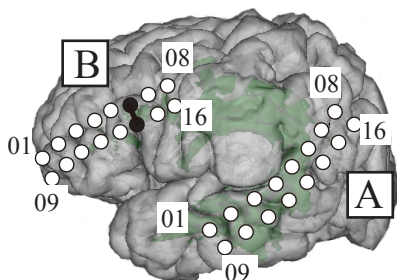
B04-12 stimulation



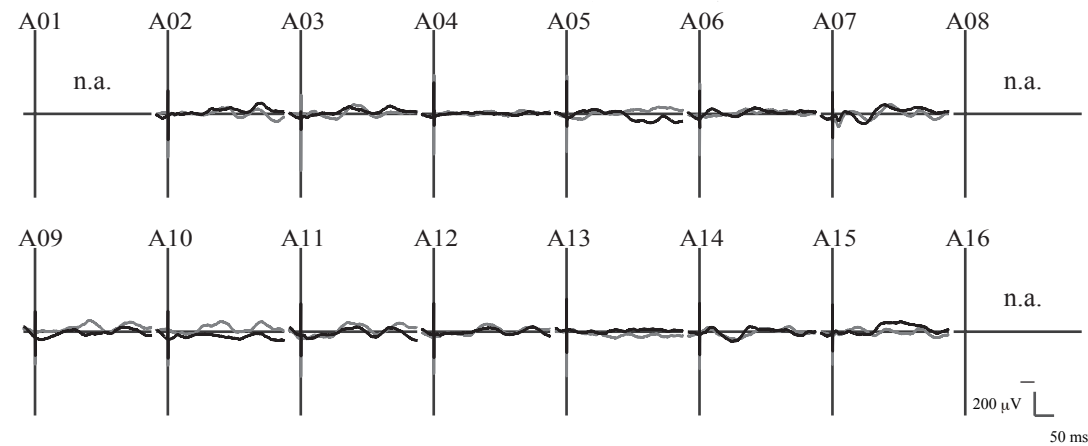
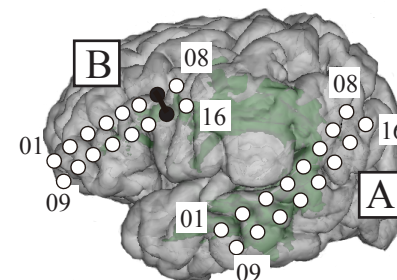
B05-13 stimulation



B06-14 stimulation

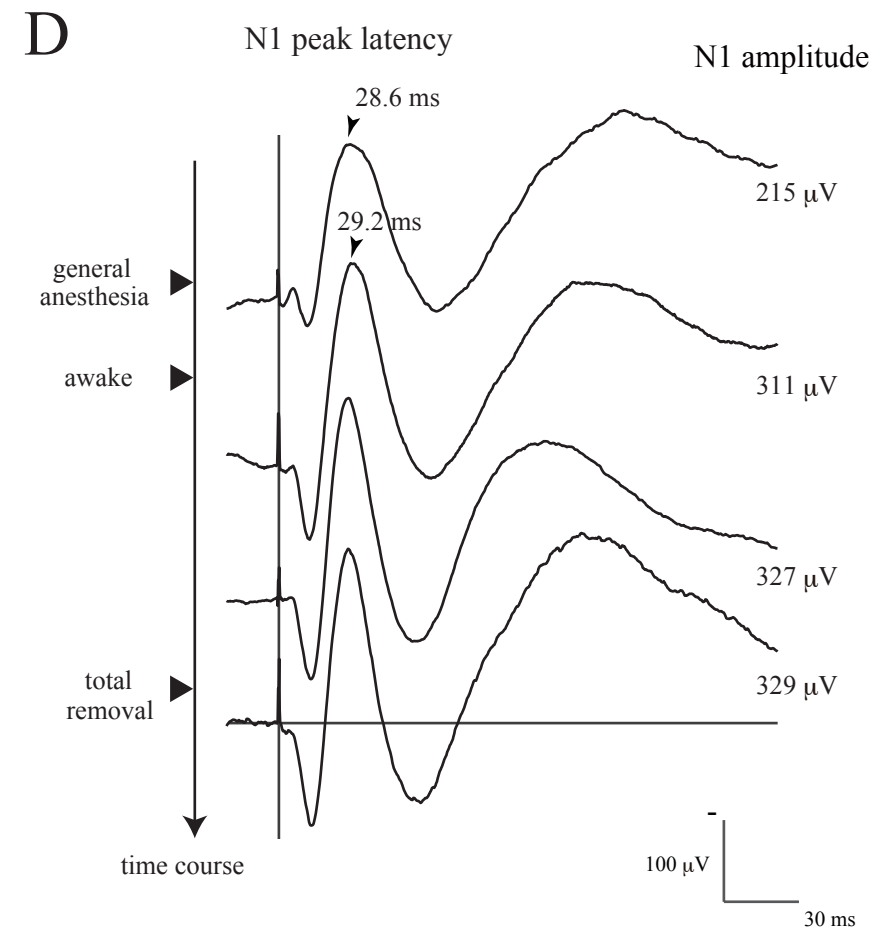
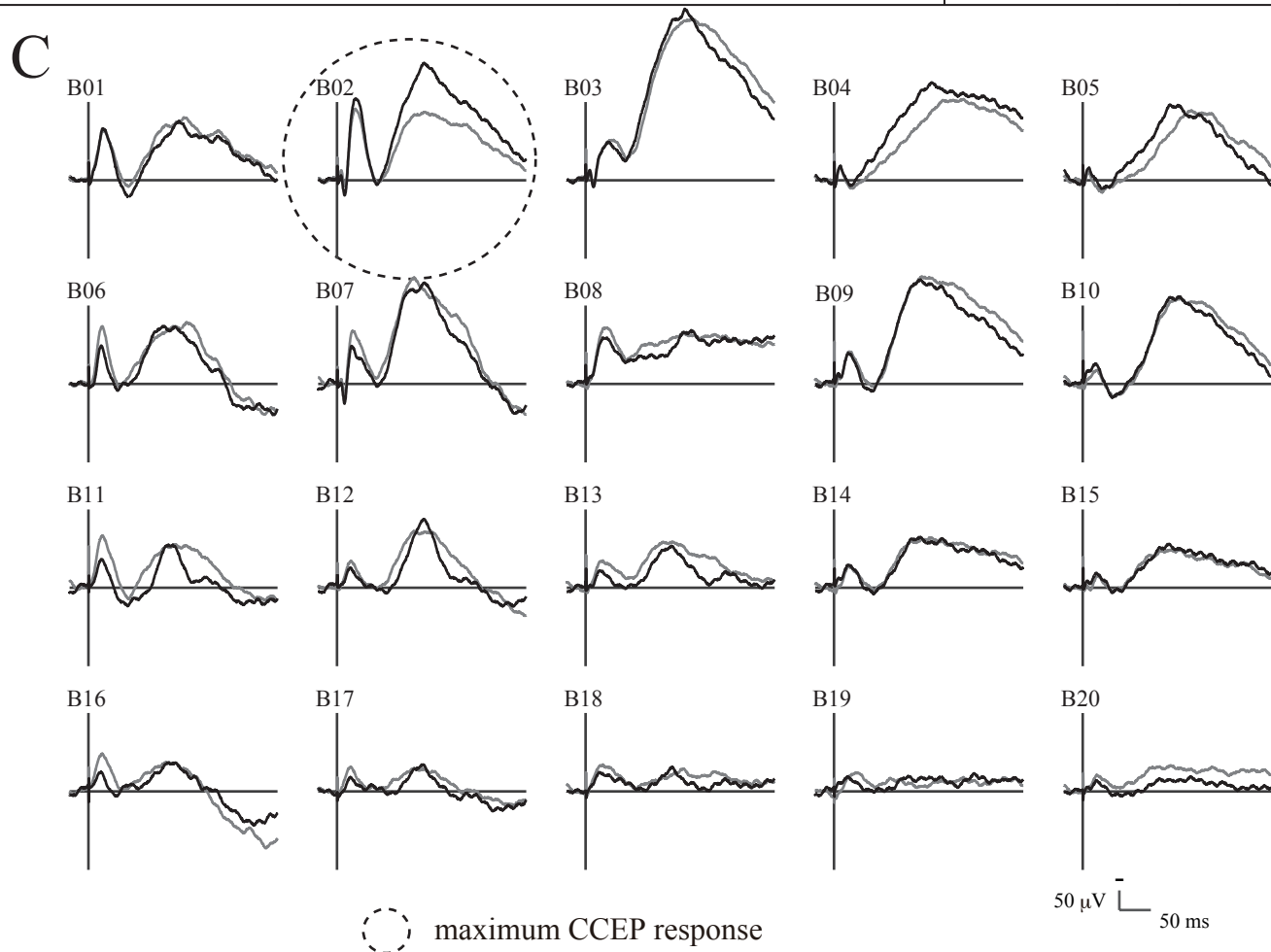
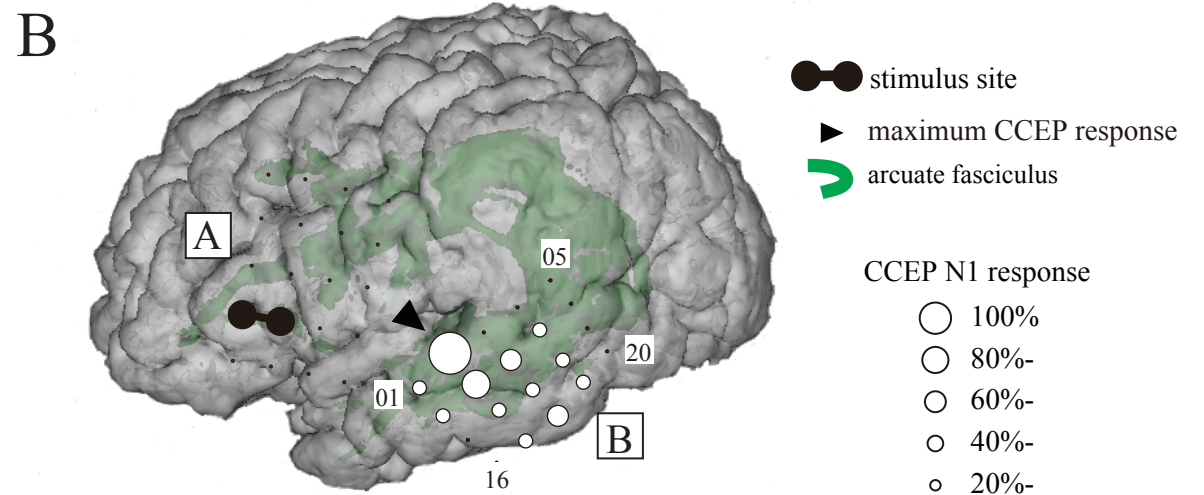
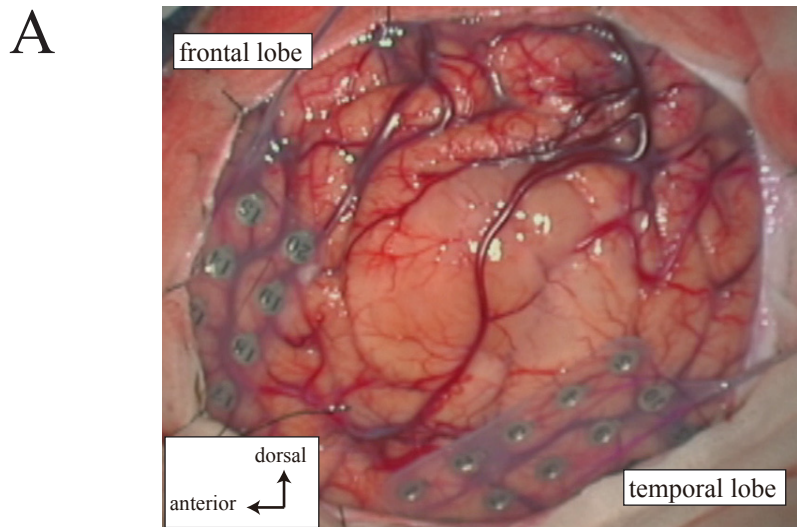


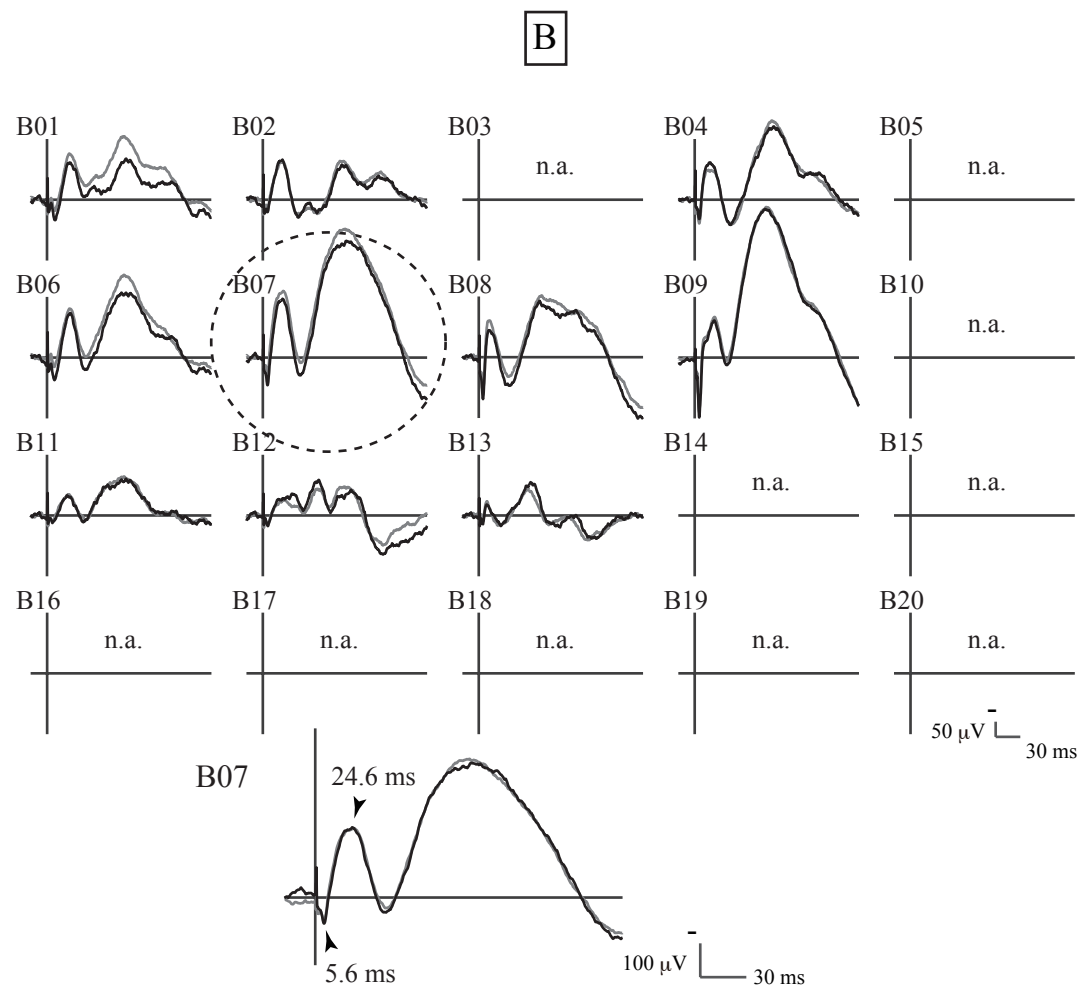
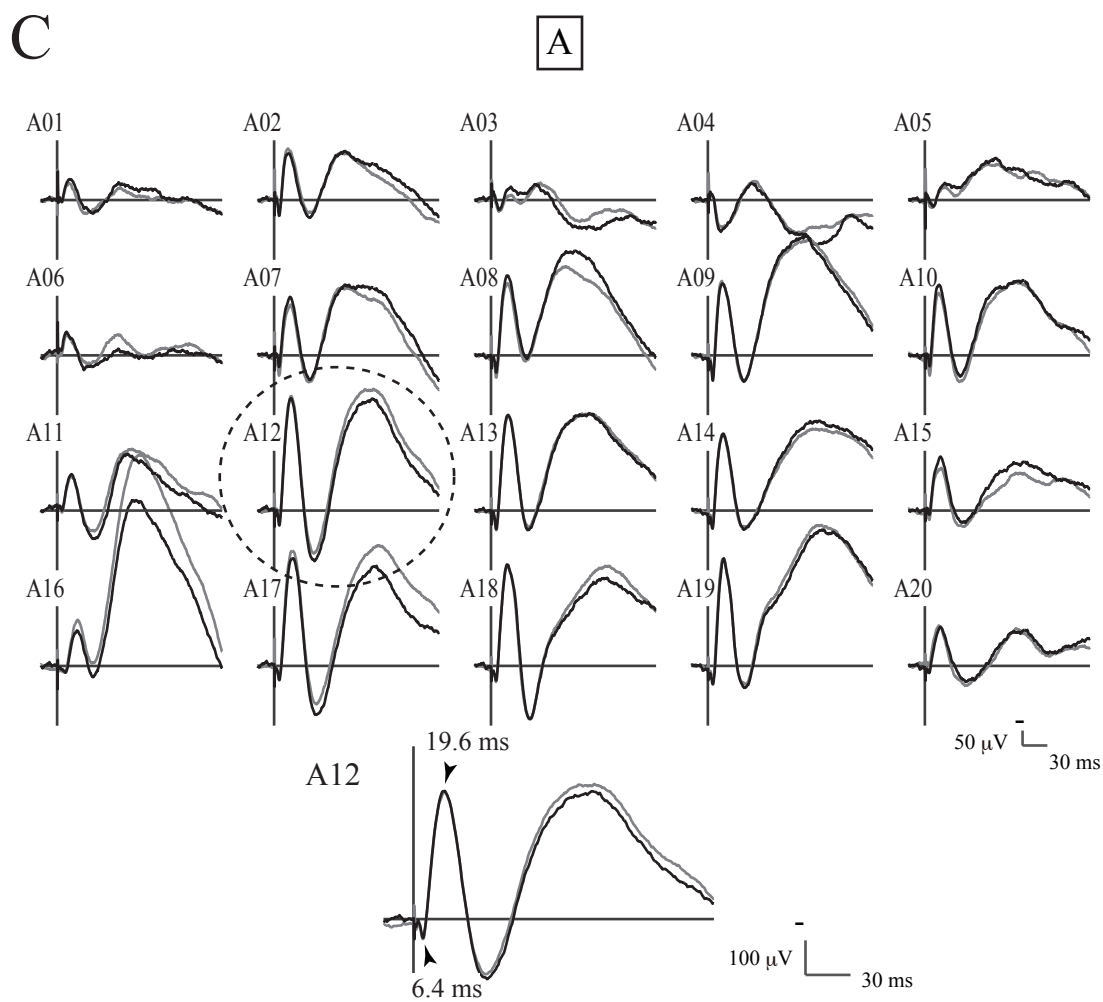
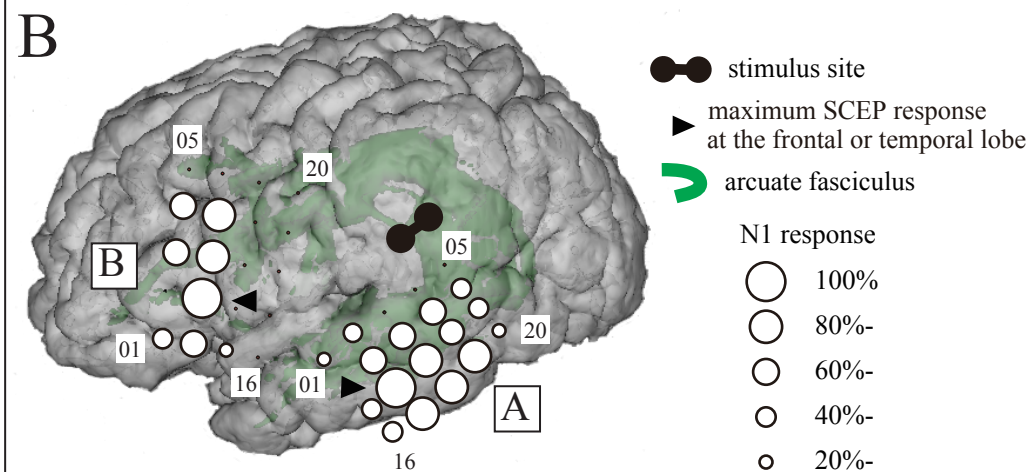
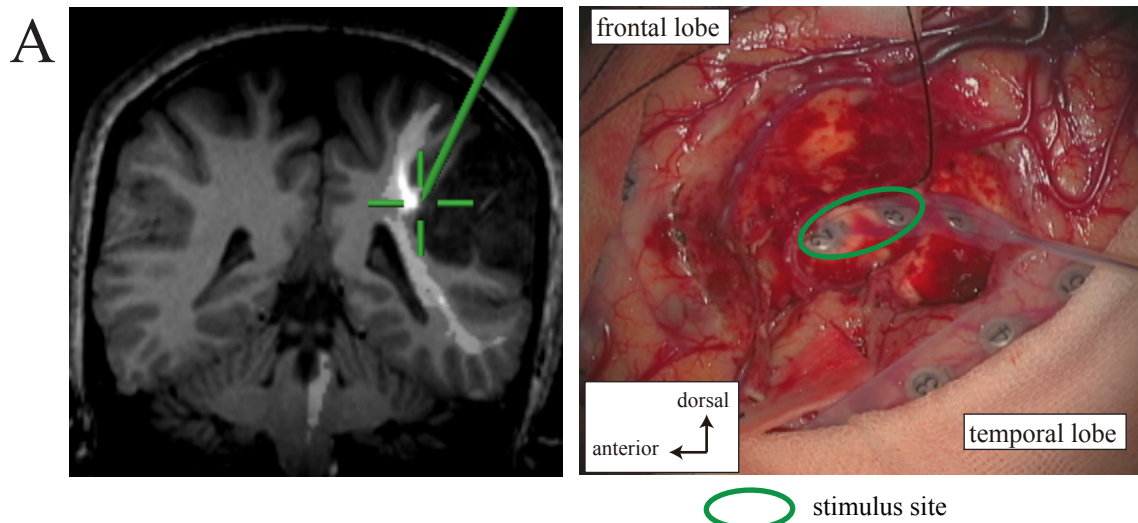
B07-15 stimulation



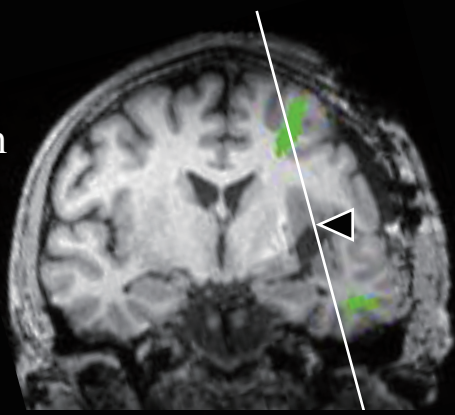
● stimulus site

➤ arcuate fasciculus

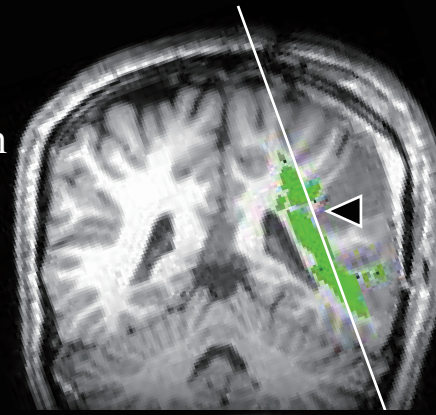




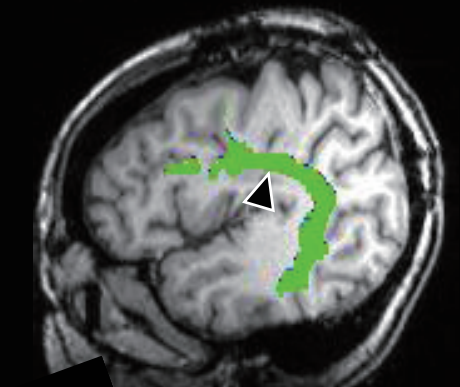
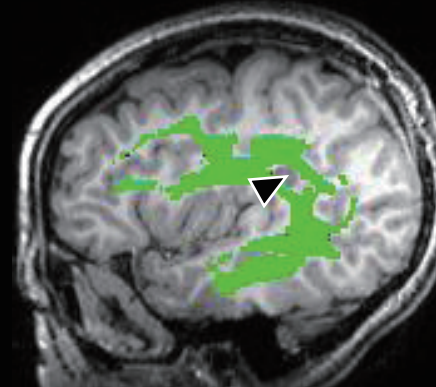
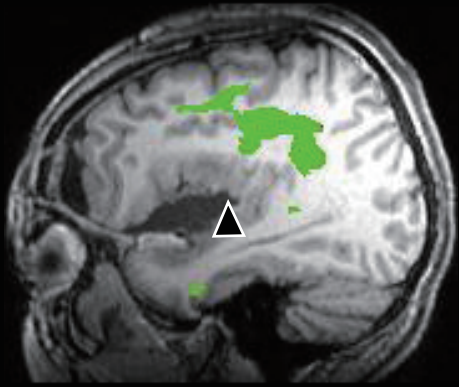
Patient 1
d = 14.9 mm



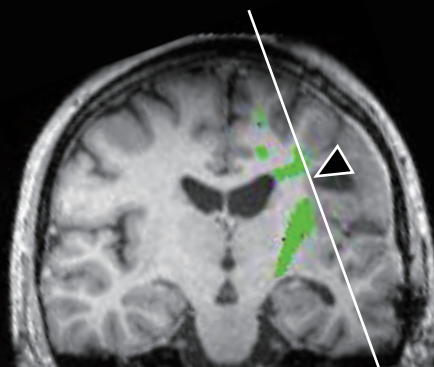
Patient 3
d = 3.0 mm



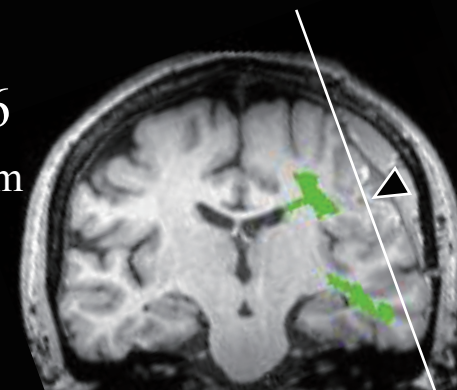
Patient 4
d = 1.4 mm





Patient 5
d = 2.8 mm



Patient 6
d = 11.2 mm



 arcuate fasciculus
 stimulus site
d = distance between
the stimulus site and
the arcuate fasciculus

